Pacific Northwest
NATIONAL LABORATORY

PNNL-29113

Baseline Evaluation of Eddy Current Testing for PWSCC Susceptible Materials

Technical Letter Report

September 2019

John P. (Jack) Lareau
Michael R. Larche
Aaron A. Diaz

Carol Nove, NRC COR

Prepared for the U.S. Nuclear Regulatory Commission
under a Related Services Agreement with the U.S. Department of Energy
CONTRACT DE-AC05-76RL01830

DISCLAIMER

PACIFIC NORTHWEST NATIONAL LABORATORY
operated by
BATTELLE
for the
UNITED STATES DEPARTMENT OF ENERGY
under Contract DE-AC05-76RL01830

Printed in the United States of America

Available to DOE and DOE contractors from the
Office of Scientific and Technical Information,
P.O. Box 62, Oak Ridge, TN 37831-0062;
ph: (865) 576-8401
fax: (865) 576-5728
email: reports@adonis.osti.gov

Available to the public from the National Technical Information Service,
U.S. Department of Commerce, 5285 Port Royal Rd., Springfield, VA 22161
ph: (800) 553-6847
fax: (703) 605-6900
email: orders@ntis.fedworld.gov
online ordering: http://www.ntis.gov/ordering.htm

This document was printed on recycled paper.
(9/2003)

PNNL-29113

Baseline Evaluation of Eddy Current Testing for PWSCC Susceptible Materials

Technical Letter Report

September 2019

John P. (Jack) Lareau
Michael R. Larche
Aaron A. Diaz

Carol Nove, NRC COR

Prepared for
the U.S. Nuclear Regulatory Commission
under a Related Services Agreement with the U.S. Department of Energy
Contract DE-AC05-76RL01830

Pacific Northwest National Laboratory
Richland, Washington 99354

Abstract

This technical letter report (TLR) summarizes technical efforts focused on assessments of eddy current testing (ET) examinations using various mockups for obtaining baseline surface and subsurface conditions on materials susceptible to primary water stress corrosion cracking (PWSCC). The scope of this work included nondestructive evaluation characterization of weld surfaces on mockups that were identified for application of various surface peening approaches. All of the work reported here was conducted prior to planned peening of these surfaces to evaluate pre-peening conditions, and subsequently compare the baseline ET results with post-peening conditions. The overall objective of this work was to demonstrate the effectiveness of employing ET for detecting near/sub-surface defects on mockups in support of peening assessments for surface stress improvement and mitigation of PWSCC in these materials.

The U.S. Nuclear Regulatory Commission has communicated their expectations to industry for eddy current inspections of peened, inlayed, and onlayed dissimilar metal welds and is interested in better understanding detection performance and sensitivity of ET techniques to support the development of a technical foundation for detection and sizing limits, effective ET qualification requirements, alternate inspections or programs for evaluating PWSCC mitigation processes, and development of ET acceptance standards that can be referenced in the appropriate American Society of Mechanical Engineers Section XI Code Case (N-770-X).

This TLR provides a technical discussion focused on the ET data obtained, the analysis, and conclusions drawn from surface examinations of various plate standards and actual components extracted from cancelled nuclear power plants.

Acknowledgments

The work reported here was sponsored by the U.S. Nuclear Regulatory Commission (NRC). Pacific Northwest National Laboratory (PNNL) would like to thank Mr. Jay Collins, Dr. Stephen Cumblidge, Ms. Carol Nove, and Mr. Bruce Lin of the NRC for their guidance and technical direction over the course of this work.

The authors also wish to thank Mr. Kevin Neill and Mr. Royce Mathews for their support of laboratory operations, mockup preparation/characterization, and data acquisition activities. In addition, the authors are indebted to Ms. Lori Bisping for all of her hard work in providing project coordination, administrative, and financial reporting support to this project. Finally, the authors would like to extend their thanks to Ms. Kay Hass for her ongoing efforts, attention to detail, and technical editing expertise in preparing and finalizing this letter report.

PNNL is operated by Battelle for the U.S. Department of Energy under Contract DE-AC05-76RL01830.

Acronyms and Abbreviations

ASME Code	ASME Boiler and Pressure Vessel Codes and Standards
ASME	American Society of Mechanical Engineers
CRDM	control rod drive mechanism
CS	cold spray
DMW	dissimilar metal weld
DT	destructive testing
ECU	energy conversion unit
EDM	electrical discharge machined
EPRI	Electric Power Research Institute
ET	eddy current testing
ID	inner diameter
ISI	inservice inspection
MRP	Materials Reliability Program
NDE	nondestructive examination or evaluation
NRC	U.S. Nuclear Regulatory Commission
OD	outside diameter
PARENT	Program to Assess the Reliability of Emerging Nondestructive Techniques
PINC	Program for the Inspection of Nickel Alloy Components
PNNL	Pacific Northwest National Laboratory
PT	penetrant testing
PWR	pressurized water reactor
PWSCC	primary water stress corrosion cracking
RPV	reactor pressure vessel
SER	safety evaluation report
SI	surface indication
SS	stainless steel
TLR	technical letter report
UT	ultrasonic testing
VI	visual indications
VT	visual testing

Contents

Figures

Tables

1.0 Introduction

Nondestructive evaluation (NDE), a key element to ensuring the safety of nuclear power plant operations, is used to examine safety-critical components for the detection of flaws in piping and welds, steam generators, nozzles, valves, pumps, and other critical component configurations throughout a nuclear power plant (EPRI 1988). Material degradation such as that caused by primary water stress corrosion cracking (PWSCC) requires effective and reliable inservice inspection (ISI) using NDE methods proven capable of detecting corrosion, cracks, or precursors to cracking (e.g., subsurface voids). PWSCC of nickel-based alloy components and welds in the reactor coolant system of pressurized water reactors (PWRs) is a significant concern because of the potential for cracking or boric acid corrosion that could lead to a loss-of-coolant accident. Regulatory requirements have been established over nearly 2 decades to develop an inspection program that proactively addresses this degradation mechanism to provide reasonable assurance of leak-tightness and structural integrity of the reactor coolant pressure boundary. Several mitigation techniques have been authorized by the U.S. Nuclear Regulatory Commission (NRC) to allow relaxation of inspection requirements because of the evaluated effectiveness of the mitigation to address PWSCC. These mitigation programs, in concert with the associated modified inspection program, provide defense-in-depth to meet the NRC goals of protecting public health and safety.

From 2012 to 2016, the Materials Reliability Program (MRP) of the Electric Power Research Institute (EPRI) submitted a series of revisions of a topical report for review to the NRC entitled, *Primary Water Stress Corrosion Cracking Mitigation by Surface Stress Improvement (MRP-335, Revisions 0 through 3)* (EPRI 2012, 2013, 2015, 2016). This series of revised reports summarized a technical basis that motivated the NRC to initiate a project to review the effectiveness of three types of surface stress improvement processes—water jet peening, underwater laser peening, and air laser peening. The purpose of the MRP reports was to provide a basis for licensees of PWRs to proactively mitigate their nickel-alloy components and welds, and subsequently modify their inspection programs for these mitigated components or welds.

The NRC staff reviewed MRP-335 Rev. 3 (EPRI 2016) and issued a Safety Evaluation Report (SER; ML16208A485) that provided conditional approval requiring that the peening coverage and depth claimed in the analysis be demonstrated by testing (Hsueh 2016). Specifically, the SER states:

> "The NRC also reviewed the MRP's deterministic analysis and performed independent calculations to determine if any missed PWSCC or fabrication flaws in the DMW from which PWSCC cracks could initiate, could threaten the structural integrity or leak tightness of the DMW. In considering such situations the NRC staff determined that the use of eddy current examinations in combination with volumetric examinations at the time of peening and in subsequent inspections provide reasonable assurance that a flaw would be detected at the time of peening or, if not, it would be detected prior to affecting plant safety, i.e., the loss of structural integrity. Therefore, given the design parameters above, the NRC staff finds that once a DMW is peened, there is reasonable assurance that cracking should not initiate. However, if initiation does occur, the inspections, identified in this SE, will provide reasonable assurance of structural integrity and leak tightness for peened DMW."

To support their review, the NRC staff required the use of laboratory resources to perform testing on realistic plant components under as close as possible in-service operational conditions. Further, the NRC staff were focusing this testing on surfaces for which access is limited or the surface condition is rough, to ensure that effective application of the peening process is possible for the range of components identified in MRP-335 Rev. 3 (EPRI 2016). This work included the use of both ultrasonic and eddy current testing (ET) techniques for baseline material characterization assessments.

The work described here provides a summary of technical efforts focused on assessments of ET examinations to obtain baseline surface condition characterization of mockups being prepped for peening evaluations. These mockups contained butt welds and J-groove welds constructed from materials susceptible to PWSCC. The scope of this work focused on characterizing the surface conditions of these mockups and weld surfaces prior to and after peening. This report aims to describe this ET research in context of NRC criteria for eddy current inspections of peened, inlayed, and onlayed dissimilar metal welds (DMWs). This report addresses the need to better understand detection performance and sensitivity of ET techniques to:

- support the development of a technical foundation regarding detection and sizing limits
- develop effective ET qualification requirements
- develop more effective alternate inspections or programs for evaluating PWSCC mitigation processes
- develop ET acceptance standards that can be referenced in the appropriate American Society of Mechanical Engineers (ASME) Boiler and Pressure Vessel Codes and Standards (ASME Code) Section XI Code Case (N-770-X).

1.1 Objective and Scope

Code Case N-770-X requires surface examinations of inlays and onlays to detect small cracks on and near the surface (ASME 2009). Additionally, as mentioned in Section 1.0, peening has been proposed by the industry as a means for surface stress improvement and as a PWSCC mitigation technique, which would necessitate similar flaw detection requirements for small cracks on and near the surface. These surface examinations may be performed using penetrant testing (PT) or ET. While the inspection requirements spell out the acceptance criteria for PT, it is not clear how these acceptance criteria may be applied to ET. Also, there is no clearly defined qualification program for ET that would satisfy the requirements of N-770-X. While ET has been demonstrated to be able to detect small surface-breaking and near-surface defects in specialized examinations, ET's capabilities are assumed as there is limited direct research on currently employed methods for detection of these defects in inlays and onlays. Because the stress improved region induced by peening and the resistant material added by inlays and onlays are very thin, it is important to ensure that the eddy current inspections are effective. This requires a better understanding of ET detection performance and sensitivity. This work will help us better understand the ability of ET to detect and size small surface-breaking and near-surface embedded flaws in butt welds, J-groove welds, and nickel-alloy inlays and onlays. The scope of this technical letter report (TLR) provides a technical discussion focused on the ET data acquired and the analysis and conclusions drawn from the surface examinations of various plate standards and actual mockups extracted from cancelled nuclear power plants.

1.2 Report Organization

The work described herein was intended to provide a summary of technical efforts focused on eddy current surface and subsurface materials characterization of appropriate mockup specimens to be used to address confirmatory research related to assessing the effectiveness of peening approaches for surface stress improvement. This TLR is organized with Section 2.0 providing the technical background and previous relevant work. Section 3.0 describes the motivation for this work, while Section 4.0 describes the laboratory evaluations conducted for assessing ET detection capability. Section 5.0 provides examples of laboratory-acquired data and discusses the results from those examinations. Lastly, a discussion is provided and conclusions are presented in Section 6.0 with technical references listed in Section 7.0.

2.0 Background and Previous Relevant Work

2.1 Overview of Eddy Current Surface Examinations

Although ET is not generally used for Code inspections of DMWs and J-groove welds, it actually has been used extensively both domestically and abroad for these applications. There is a relatively small population of flaws detected by ET that have other confirmatory data (PT or destructive testing [DT]). However, the available data is very positive for demonstrating the validity of the technique for this application.

Eddy current testing for surface examinations is described in ASME Code Section XI, Appendix IV, Eddy Current Examination (ASME 2017). The qualification requirements for piping and vessel inspections are documented in Supplement 2. In summary, this supplement specifies a calibration notch 0.5 mm (0.020 in.) deep and less than 0.25 mm (0.010 in.) wide (typical of an electrical discharge machined [EDM] notch) or a compressed notch 1.02 mm (0.040 in.) deep. The qualification notches are not to exceed the allowable length specified in ASME Code Section XI IWB-3514 for piping. However, because ASME Code Section XI has no allowable surface flaw lengths for weld material susceptible to PWSCC (Alloy 600, Alloy 82, and Alloy 182), IWB-3514 does not cover examinations of the wetted surface of susceptible materials.

However, ASME Code Section XI IWB-3514.1 allows wetted surface planar flaws that are detected by a preservice volumetric inspection. This section specifically includes PWSCC-susceptible material. The governing table for allowable flaw lengths is IWB-3514-2, which allows surface-connected flaws less than 6.35 mm (1/4 in.) for wall thicknesses greater than or equal to 50.8 mm (2 in.). Paragraph IWB 3514.8 requires additional ISI on a shorter interval to monitor potential flaw growth. Because ASME Code Section XI allows for additional confirmatory inspections to refine flaw measurements, one could argue that the 6.35 mm (1/4 in.) acceptance length is a de facto allowable flaw using surface ET.

In Sweden, ET of primary system safe-end welds is commonly performed. The Swedish inspection requirements include detection of a 1 mm (0.04 in.) deep by 6 mm (0.24 in.) long flaw on the wetted surface. In order to meet this requirement, ET was demonstrated and is the preferred method to supplement the standard volumetric ultrasonic inspection (Söderstrand 2003).

In the United States, ET has been used extensively for base metal inspections of Alloy 600 control rod drive mechanism (CRDM) penetration nozzles. Because the emphasis of this report is the inspection of weld metal, base metal ET will not be discussed.

There has also been considerable work in the United States using ET for Alloy 82 and Alloy 182 welds on both CRDM partial penetration J-groove welds and DMW safe-end welds. Pacific Northwest National Laboratory (PNNL) has conducted confirmatory evaluations of techniques using CRDM nozzles removed from the North Anna Unit 2 retired reactor vessel head. In addition, the Program for the Inspection of Nickel Alloy Components (PINC) and the follow-on study, Program to Assess the Reliability of Emerging Nondestructive Techniques (PARENT), reviewed results from ET inspections of DMWs and J-groove welds. Each of these reports indicates that ET is an effective method for detecting PWSCC in pipe welds.

Though ET has been shown to be effective at detecting PWSCC in piping welds, challenges remain for ET of J-groove welds including incomplete coverage in areas of tight access such as the downhill sides of nozzles. Further, at an NRC public meeting on September 9, 2014, utility representatives shared concerns regarding potential false positives leading to unnecessary, time-consuming repairs (Crooker et al. 2014). As will be described below, PNNL addressed these concerns as well as an additional issue of potentially missing near-subsurface flaws (which had been identified as the cause of leakage in bottom-mounted nozzles with a similar J-groove weld design).

On the coverage issue, PNNL purchased commercially available ET probes that had been used for field inspections and confirmed that the region at the toe of the weld, especially on the downhill side, could not be accessed with these probes (see Section 5.0) because of the mechanical interference. To overcome this limitation, a flexible, conformal bobbin probe that is commonly used in aerospace applications was purchased, and it was demonstrated that this probe design could access this region. However, there were limited samples available to perform a detailed assessment of detection capability.

On the issue of false positives, discussions were held with utility and inspection vendors to better understand relevant ET field experience with J-groove welds. From these discussions one inspection was identified that resulted in at least three ET calls not being confirmed by PT. However, a lack of PT confirmation does not necessarily translate to a false positive ET conclusion as demonstrated by the DT performed as part of the North Anna Unit 2 assessments performed by Cumblidge et al. (2007). This work showed that PT missed flaws that were detected by ET and confirmed by DT.

To determine the detectability of near-subsurface flaws (assumed to be voids or slag from welding), mockups were made with simulated voids and then coated with Alloy 625 (Inconel) to create surface ligaments ranging from 0.5–1.5 mm (0.02–0.06 in.). The probe that had been used for most inservice inspections of J-groove welds and the flex probe were capable of detecting these welding flaws. However, for the probe that has been used in field inspections, these anticipated flaws are in the same location as the inaccessible zone at the toe of the weld.

2.2 NRC Expectations for Eddy Current Inspections of Peened, Inlayed, and Onlayed Dissimilar Metal Welds

In Cumblidge (2015), the NRC communicated their expectations to industry for eddy current inspections of peened, inlayed, and onlayed dissimilar metal welds. The NRC listed several expectations to ensure a better understanding of detection performance and sensitivity of ET techniques to support the development of a technical foundation for detection and sizing limits, effective ET qualification requirements, alternate inspections or programs for evaluating PWSCC mitigation processes, and development of ET acceptance standards that can be referenced in the appropriate American Society of Mechanical Engineers Section XI Code Case (N-770-X). These expectations included:

- “Eddy current acceptance standards that have a technical basis given the sizes and depths of flaws that can challenge a peened surface and/or an Alloy 52 inlay or onlay”
- “Eddy current qualification requirements that provide confidence that the procedure can reliably detect shallow and near-surface flaws and be able to discriminate between shallow flaws and scratches and weld passes”

- “Alternate inspection methods or programs to determine if the mitigation process is functioning as intended.”

In the limited effort documented in this report, these expectations have not been rigorously addressed, but these points are considered in later sections.

2.2.1 Acceptance Standards

Surface examination preservice acceptance standards (for ET) are based solely on length, do not address depth, and are found in ASME Code Section XI IWB-3514.1. Allowable linear flaw lengths for austenitic steels can be found in Table IWB-3514-2. Depth can be addressed indirectly as a detection threshold but cannot be evaluated quantitatively. One approach for determining the necessary detection sensitivity for ET examinations is to consider it in terms of the percentage of the peening depth, which is claimed to be at least 1 mm (0.04 in.) in MRP-335 Rev. 3. Both MRP-335 Rev. 3 and the associated SER assume a flaw 90% of the peening depth with a length-to-depth ratio of 4.25. ASME Section XI Appendix IV specifies a 0.5 mm (0.02 in.) deep EDM notch for the calibration flaw. Although an EDM notch is a non-conservative representation of PWSCC, this sensitivity associated with this notch has been shown to be capable of detecting actual PWSCC that has been confirmed by DT (discussed in more detail in Section 2.5 and its subsections). Additionally, prior experience with steam generator tube inspections, which employ a very similar ET method as has been proposed for DMWs, indicates that this flaw size would be readily detectable.

2.2.2 Detection of Near Subsurface Flaws and Discrimination Between Cracks and Scratches

The standard practice for discriminating scratches from PWSCC is to assess how linear the flaw indication is. In general, actual surface scratches are relatively long and straight compared to cracking. In practice inspecting CRDM nozzles, for example, many indications have been identified as scratches and none have been reported to have grown in subsequent inspections. Various surface gouges also occur from manufacturing, and these are easily distinguished from actual cracks. The + Point or X-Point probe responds with opposite signal polarity for circumferential or axial flaws. When both polarities occur in the same signal, the indication is determined to be from a volumetric, non-crack-like condition. The minimum depth detection capability was not specifically addressed; however, there is a large body of data based on steam generator tube inspections that supports a detection threshold of 0.25 mm (0.010 in.), based on 20 percent of a typical tube wall thickness. Therefore, if the defect is less than 0.25 mm (0.010 in.), detection would be questionable in weld material. In plate material, flaw detection at 0.13 mm (0.005 in.) has been demonstrated. Although weld metal has an intrinsically higher background noise, the + and X-Point coil configurations suppress the local variations in conductivity/permeability so that they are effective for inspecting the anisotropic material associated with high nickel-alloy welds.

2.2.3 Alternate Inspection Methods or Programs

The available literature indicates that ET is more effective at detecting surface-breaking PWSCC flaws in comparison to PT, visual testing (VT), and various ultrasonic and potential drop methods (Cumblidge et al. 2007; Cumblidge et al. 2010). For near-subsurface flaws, the only available work is from the PNNL peening project simulations as described in Section 2.2.1. As for alternative inspection programs, this has been addressed in ASME Code Section XI IWB 3514.8 and MRP-335 requiring repeat ISIs after a few operating cycles.

2.3 PNNL Research – North Anna Unit 2 Removed CRDM Weld

PNNL-16628, *Nondestructive and Destructive Examination Studies on Removed from Service Control Rod Drive Mechanism Penetrations* (Cumblidge et al. 2007), reports on the results of NDE and DT of CRDM penetration #31 removed from North Anna Unit 2, which had clear leakage from the primary system to the outer surface of the reactor vessel head. The actual leaking crack was entirely within the Alloy 182 weld and buttering and did not extend into the nozzle base metal. The leaking crack was determined to have a surface length of 6 mm (0.24 in.) with the subsurface length expanding to the entire cross section of the weld (~25 mm or 1 in.) and a few millimeters deep into the weld. ET was the only inspection method that detected this flaw, as PT, VT, and ultrasonic testing (UT) methods were not successful.

PNNL-16628 concluded: "ET was able to detect the through-weld crack, all cracks that were detected using PT and verified with VT, and others that were detectable only with ET. ET was the most useful technique for finding PWSCC on the J-groove weld and showed much higher sensitivity than any of the other techniques."

2.4 PINC and PARENT

NUREG/CR-7019 (Cumblidge et al. 2010) reports on the results from the PINC program addressing NDE of high nickel-alloy welds. Both piping welds (DMWs) and J-groove welds were simulated in laboratory mockups. Also, in addition to the efforts on laboratory mockups, information from the removed CRDM J-groove weld from North Anna Unit 2 is included. Several NDE methods were evaluated including both volumetric and surface inspections. Surface inspections included ET, PT, and VT-1. The volumetric examinations included conventional UT and phased-array UT.

NUREG/CR-7019's conclusions indicate that among the various ET coil designs used, a single cross-wound ET coil scanned over the entire susceptible material is the most effective technique for detecting surface flaws in both DMWs and J-groove welds. The laboratory effort described in Section 5.0 used the same coil design as was reported to be the best choice among ET coil designs in PINC and PARENT activities.

The laboratory-performed ET and DT results are provided in Table 2.1 and Figure 2.1 (extracted from the NUREG/CR-7019; Table 7.1 and Figure 7.9). In Table 2.1, there are a total of 16 ET flaw-like indications reported and only 6 were confirmed as actual PWSCC. At first glance, this would seem to indicate a high false positive call rate. However, the laboratory ET technique differed significantly from the actual field ISI method in both calibration approach and analysis guidelines. The two major differences were the calibration flaw (4 mm vs. 1 mm; 0.16 in. vs. 0.04 in.) and the analysis guidelines used in the field to discriminate crack-like signals from non-relevant indications, such as scratches and geometric artifacts. For the field results, documented prior to the PNNL study, the six confirmed PWSCC locations were identified and the remaining "false positives" were not flagged as crack-like indications. Therefore, the field techniques would have fewer false calls because of how the field calibration is conducted and how the data are analyzed.[1] This will be discussed further in the field experience section with the North Anna Unit 2 field inspection.

[1] The vendor's analysis guidelines include designations for surface indications (SI), which are considered to be scratches, volumetric indications (VI), which are non–crack-like indications, and axial or circumfer-

The confirmed flaws ranged in length from 7 mm to 14 mm (0.28 in. to 0.55 in.). The calibration notch used for this study was a 4 mm (0.16 in.) EDM notch. EDM notches at this depth range would have a much wider opening than the ASME Code-specified less than 0.25 mm (0.010 in.) because the EDM process will arc to the sides of the electrode at increasing depths. The study also had 1.0 mm and 0.5 mm (0.4 in. and 0.2 in.) deep EDM notches, which are more representative for evaluating cracks. The deeper notch was also being used to assess ultrasonic responses.

Table 2.1. ET Results from a Removed J-groove weld from North Anna Unit 2 CRDM #31

Table 7.1 North Anna Unit 2 Eddy Current Responses and Destructive Validation (Cumblidge et al. 2010)

Indication	Angle	Length	Max Voltage	% EDM Notch	Confirmed PWSCC?	Depth[(a)]
1	45°	2 mm (0.08 in.)	2.1	20%	No	< 6 mm (0.24 in.)
2	50°	5 mm (0.2 in.)	1.9	18%	No	< 6 mm (0.24 in.)
3	55°	4 mm (0.16 in.)	3.3	32%	No	< 6 mm (0.24 in.)
4	65°	2 mm (0.08 in.)	1.8	18%	No	< 6 mm (0.24 in.)
5	70°	4 mm (0.16 in.)	2.2	21%	No	< 6 mm (0.24 in.)
6	75°	3 mm (0.12 in.)	2.5	24%	No	< 6 mm (0.24 in.)
7	80°	3 mm (0.12 in.)	2.3	22%	No	< 6 mm (0.24 in.)
8	130°	4 mm (0.16 in.)	2.3	22%	No	< 6 mm (0.24 in.)
9	145°	10 mm (0.4 in.)	3.2	31%	Yes	< 25 mm (1.0 in.)
10	155°	8 mm (0.32 in.)	3.3	32%	Yes	Through-Weld Leaking
11	160°	14 mm (0.55 in.)	4.1	40%	Yes	< 25 mm (1.0 in.)
12	170°	5 mm (0.2 in.)	2.6	25%	No	< 6 mm (0.24 in.)
13	200°	8 mm (0.32 in.)	4.6	45%	Yes	< 25 mm (1.0 in.)
14	215°	10 mm (0.4 in.)	1.8	18%	No	< 6 mm (0.24 in.)
15	225°	9 mm (0.35 in.)	4.6	45%	Yes	< 25 mm (1.0 in.)
16	255°	7 mm (0.28 in.)	4.2	41%	Yes	Through-Weld Not Leaking

(a) Note that the Depth column only refers to sample cutting locations and is not an indication of flaw depth.

ential indications (AI or CI, respectively), which are considered to be crack-like indications. The SI designation is for signals with low amplitude and phase, which indicates no depth. With a + Point probe design, one coil will create a signal with a negative phase and the other will produce a positive phase response, which may indicate either an axial or circumferential crack-like indication. For VIs, from one scan index to another, either coil may detect the flaw first, producing signals that can alternate between positive and negative phase, which are classified as VI. In addition, with the instrument used (IntraSpect ET Data Acquisition System), there is a signal processing approach that provides a spatial derivative of the signal response, which reduces the background noise from low spatial frequency effects, such as conductivity and geometry variations. This feature has been demonstrated to reduce false positive calls.

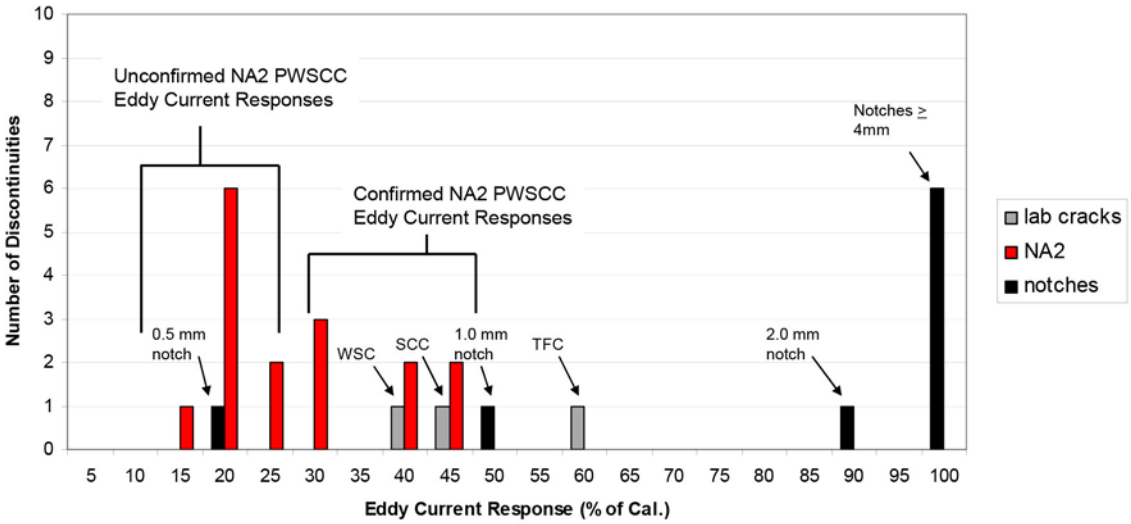

Figure 2.1. Number and Amplitude of Non-relevant Indications (unconfirmed by DT), Actual PWSCC, and Laboratory-Produced Cracks as Compared to Various Notch Sizes. All the confirmed PWSCC responses exceed the response from the ASME Code-specified calibration notch depth (0.5 mm; 0.020 in).

2.5 Relevant Field Experience

A number of ET inspections have been performed in the United States and abroad. In accordance with NRC Order 003-09 (Borchardt 2004) regarding reactor vessel upper head penetrations, utilities had the option of performing a volumetric inspection (UT) of the penetration nozzle or a surface inspection (PT or ET) of the susceptible wetted surface regions of the penetration nozzle and J-groove weld as shown in Figure 2.2. Some utilities elected to perform both UT of the nozzle and ET of the wetted surface. The North Anna Unit 2 plant was one site where extensive ET of the J-groove weld was performed and several crack-like indications were reported. Because ET of DMWs is not generally conducted because of a lack of acceptance criteria in the ASME Code and there are no performance demonstration protocols, these inspection capabilities are documented via technical justifications provided by the various inspection vendors. One of the significant limitations for inspecting J-groove welds, especially with a steep side-hill angle, is the geometric obstruction at the toe of the weld. This will be discussed further in the laboratory work section.

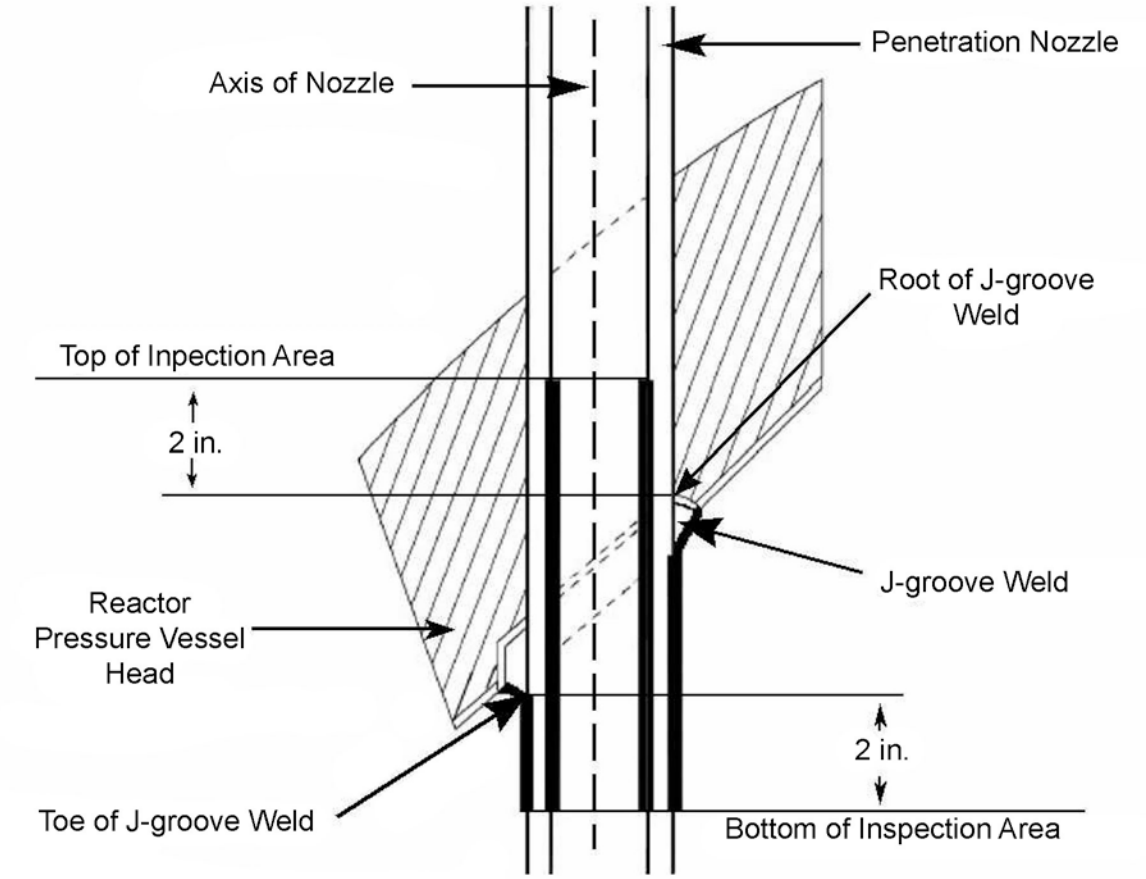

Figure 2.2. Wetted Surface Inspection Coverage Requirements in Accordance with NRC Order 003-009 Rev. 1. Note that the entire J weld and buttering surface are in the required inspection zone. Portions of the nozzle base metal on the inner diameter and outer diameter are also included, but these regions are not the subject of this report.

2.5.1 North Anna Unit 2

As mentioned above, the North Anna Unit 2 inspection included extensive ET inspections of the penetration nozzle inner diameter (ID) and portions of the J-groove weld. The field inspection used an X-Point probe (cross with probe rotated to 45°). Several J-groove welds were reported to have crack-like indications.

CRDM penetrations #31 and #59 were sent to PNNL for DT. CRDM #31 was evaluated for flaw detection capability in the J weld. CRDM #59 also had two crack indications reported in the field data, but these were not evaluated destructively because the emphasis for this nozzle was evaluating leak path detection in the annulus between the nozzle and vessel head above the J weld. The DT results from a PNNL study confirmed six PWSCC indications ranging from 5.59 mm to 9.65 mm (0.22 in. to 0.38 in.) in length. Several surface imperfections are also evident in Figure 2.3 (Lareau and Adamonis 2003), but these were all evaluated as non-crack-like in the field results. The PNNL reports also indicated that most, but not all, of the ET indications were detectable by PT. The surface-connected crack portions were reported to be associated with hot tears and had a tendency to have a very small crack opening displacement. This could have been further complicated by the surface decontamination process, which could

result in smearing the surface metal and closing the crack opening further. In general, the field results show a good correlation between PT and ET when both have been performed in situ (Cumblidge et al. 2007; Cumblidge et al. 2010).

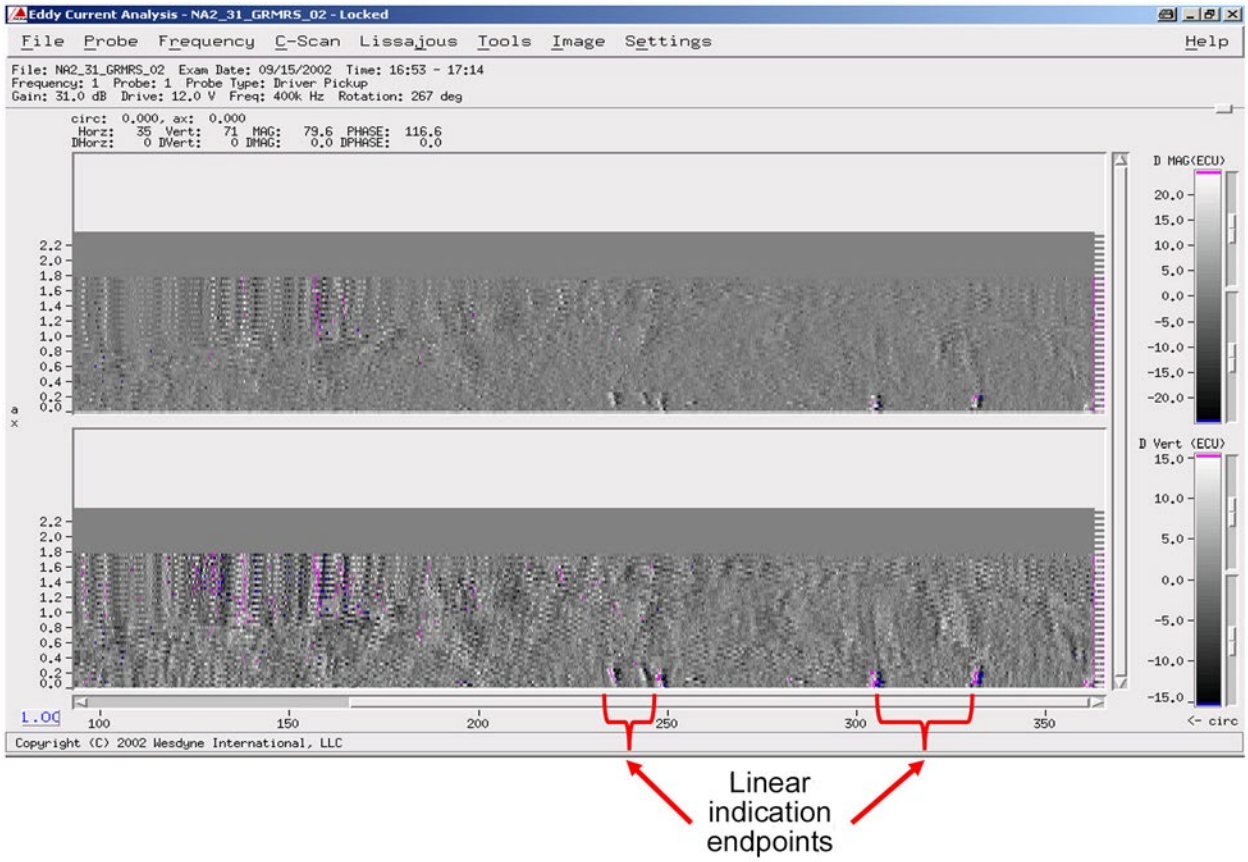

Figure 2.3. North Anna Unit 2 CRDM #31 J-Groove Weld ET Results from the Field Inspection. Three crack-like indications were identified around 250°, one each at approximately 310°, 340°, and 360°, consistent with the DT results. (Since PNNL data are not provided here, and the North Anna zero reference point differs from the PNNL study, the angular position shown here does not agree with the locations given in Table 2.1.)

It is important to note that these surface-connected flaws were found in the buttering region of the weld. It is apparent in the data that this region was ground in the factory, while the actual J-groove weld surface was as-welded and correspondingly rougher. This has been reported as unique to the particular manufacturer. Other manufacturers grind the J-groove weld surface as well.

2.5.2 Davis Besse J-Groove Weld Inspection (2010)

An extensive inspection of J-groove welds was conducted at Davis Besse after boric acid leakage was detected on the reactor vessel head (Boland 2010). VT, ET, and PT were conducted on several nozzles. In particular, with two J-groove welds that were examined (nozzles 40 and 66), the ET and PT results did not agree. (Note that not all nozzles that had an ET inspection also had a PT confirmation due to different selection criteria for testing.) Nozzle 40 had a linear circumferential flaw called by ET, and PT showed a 3.18 mm (1/8 in.) rounded

indication at essentially the same location. Nozzle 66 had an axial indication called by ET and a 3.18 mm (1/8 in.) rounded indication from PT, but at a different circumferential location. No DT was performed to determine which calls were correct, but there was a discrepancy between the ET and PT results for this inspection on multiple nozzles.

2.5.3 V.C. Summer Safe-End Weld

A safe-end DMW was found to be leaking at V.C. Summer in 2000, and this weld was removed and replaced. The ISI included UT and ET from the ID. The ET technique was based on using the calibration guidance of ASME Code Section XI Appendix IV, using a 0.5 mm (0.020 in.) deep EDM notch. The removed weld was evaluated using destructive methods. A limited summary of these results was presented by Westinghouse during the EPRI International Pressurized Water Reactor Materials Reliability Conference and Exhibition in 2010 and one slide is reproduced in Figure 2.4 (Lareau and Adamonis 2003).

As stated in Figure 2.4, the reported ET indications were confirmed by DT to be PWSCC; however, the actual lengths have not been reported publicly. Note that each flaw had a signal amplitude response greater than 30% of the reference notch and was detectable on at least three pixels, which is typically an increment of 1 mm (0.04 in.). The flaw orientation and the scan direction were both axial, based on the provided image. It was also reported in this presentation that none of the single- or double-pixel indications were real flaws. Based on this limited amount of data, a detection limit of 3.18 mm (1/8 in.) appears achievable. Having a length threshold for detection has been shown in field experience to be important for reducing false positive calls.

2.5.4 Japanese Experiences

Nuclear Engineering Ltd. (NEL) and Kansai Electric made a presentation on steam generator safe-end cracking events that occurred in multiple PWRs at a Nuclear Energy Institute (NEI)-Lessons Learned – World Outages Conference in 2008 in Arlington, Virginia, that was attended by a PNNL staff member. The NEL presentation detailed PWSCC events including ET results for Mihama 2 (2007), Takahama 2 (2007), and Takama 3 (2008) for DMWs in steam generator safe ends. The licensee had planned to perform ultrasonic shot peening on the Mihama 2 steam generator safe-end welds as a preemptive mitigation approach, and an ID surface ET was performed prior to the planned peening to assess the pre-peened surface condition.

At Mihama 2, 13 ET indications were reported and all were confirmed by PT and surface replication. Twelve of these indications were axial cracks in the DMW and one was a shallow crack at the edge of the stainless safe end immediately adjacent to the DMW. The measured flaws lengths ranged from 4 mm to 18 mm (0.16 in. to 0.71 in.), as presented by Kansai Electric Co., and shown in Table 2.2. Note that only 5 of the 13 indications (Δs) were detectable by UT and only 1 (#4) was sufficiently deep to allow UT depth sizing. All of the ET indications were confirmed by PT.

Based on other public presentations, the ET technique used in Japan was an array probe rather than a scanned + Point probe generally used in the United States; however, reported comparisons of these methods indicate comparable detection capability for geometries such as safe-end welds and steam generator tubes.

V. C. Summer Safe End Weld ET Results

- ET response of safe end alloy 182 weld with axial PWSCC
- DT confirmed PWSCC
- All flaws produced signals >30% reference
- All flaws were detected on a minimum of three scans

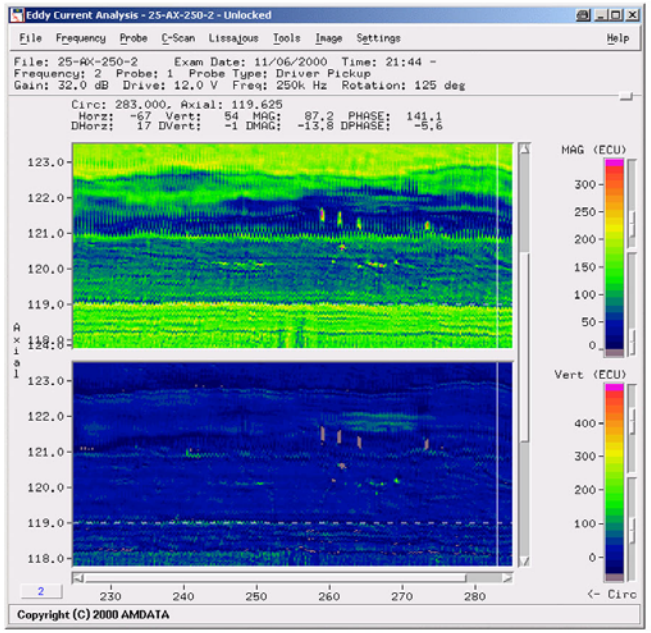

Westinghouse

5

Figure 2.4. In-Service ET Results for Safe End “A” at V.C. Summer Showing Crack Indications Detected in the DMW. DT confirmed the ET results. From Lareau and Adamonis (2003).

Table 2.2. In-Service ET Results for a DMW Steam Generator Safe-End Weld at Mihama 2 and Confirmed by PT.

Indication No. (Crack No.)	Location	Length by ECT		Depth by UT		
		Axial Direction	Circ. Direction	Circ. Shoot	Axial Shoot	
1	Groove Weld	6.0 mm	—	○	—	
2		7.0 mm	—	Δ	—	
3		9.0 mm	—	○	—	
4[a]		18.0 mm	—	× (13 mm)	—	Maximum indication in weld
5		6.0 mm	—	○	—	
6		4.0 mm	—	Δ	—	
7		6.0 mm	—	○	—	
8		6.0 mm	—	○	—	
9		6.0 mm	—	○	—	
10		6.0 mm	—	○	—	
11		6.0 mm	—	Δ	—	
12		12.00 mm	—	Δ	—	
13	Safe-end	—	4.1 mm	—	○	Indication in SS316

○ = No indication; Δ = Indications (incapable of depth sizing); × = Indication with depth sizing

(a) Only crack # 4 could be evaluated by UT to be about 30 mm deep. (The depth of other cracks could not be evaluated by UT. PT of A-steam generator inlet nozzle weld detected 23 indications in addition to 13 indications of ECT. (The 23 indications seem to be shallow cracks below the ECT-detectable limit.)

As a result of the Mihama 2 inspection crack detections, the Japanese regulator required ID surface inspections of steam generator safe-end welds. Limited ET results have been presented for Mihama 2, Takahama 2, and Takahama 3 (see Table 2.3). In addition to the Mihama 2 indications, a total of 41 ET indications were reported at Takahama 2 and 3. Only the maximum length flaws were reported, so there is no publicly available minimum length detection outside of the 4 mm (0.16 in.) flaw reported at Mihama 2. These results demonstrate that ET is a reliable detection method for PWSCC under field conditions.

Table 2.3. In-Service ET Results for Three Japanese Plants with Confirmed PWSCC in DMWs in Steam Generator Safe Ends.

Plants	SG	ECT Indications	UT Results
Mihama-2	A-inlet	13 locations	Up to 18 mm in length and 13 mm in depth
	B-inlet	No indication	—
Takahama-2	A-inlet	3 locations	Not detected
	B-inlet	2 locations	Up to 7 mm in length and 6 mm in depth
	C-inlet	4 locations	Up to 14 mm in length and 8 mm in depth
Takahama-3	A-inlet	7 locations	Up to 28 mm in length and 9 mm in depth
	B-inlet	16 locations	Up to 38 mm in length and 15 mm in depth
	C-inlet	9 locations	Up to 14 mm in length and 9 mm in depth

ECT indications at Takahama-2	ECT indications at Takahama-3
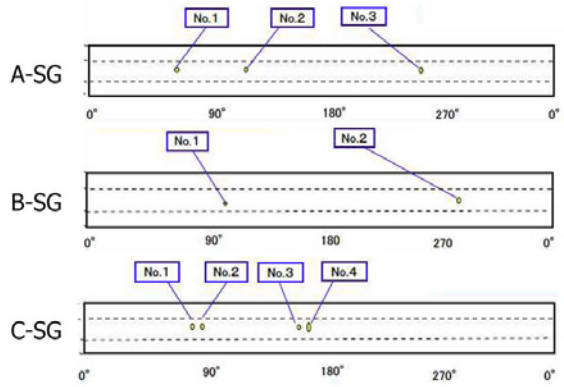	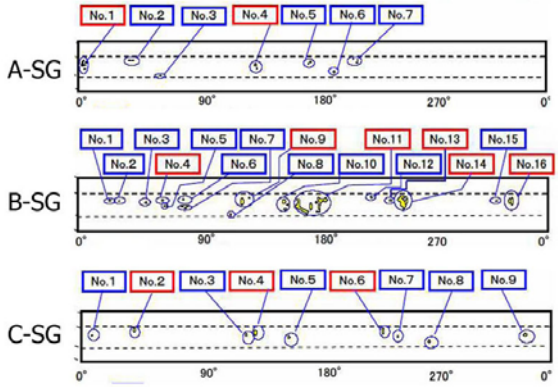

2.5.5 St. Lucie Pressurizer

A pressurizer was replaced at the St. Lucie plant and the retired component was available for post-removal NDE evaluations. Several relatively deep circumferential flaws were initially reported by various UT methods in one pressurizer nozzle. Further evaluations were performed using ET, PT, and DT on the suspect nozzle. The ET results were reported at an EPRI conference in Colorado Springs in 2010, where a PNNL staff member participated. These results are shown in Figure 2.5. These indications, unlike most field-detected flaws in Alloy 82/182 welds, were circumferential in orientation. ET and PT both reported these indications, which were determined to be weld hot tears upon DT ranging in length from 5.6 mm to 9.65 mm (0.22 in. to 0.38 in.), based on an excerpt from the DT report that was submitted to the NRC (Weakland 2008). Multiple geometric indications are apparent in Figure 2.5, but the analysis guidelines were able to discriminate against these as non-crack-like indications.

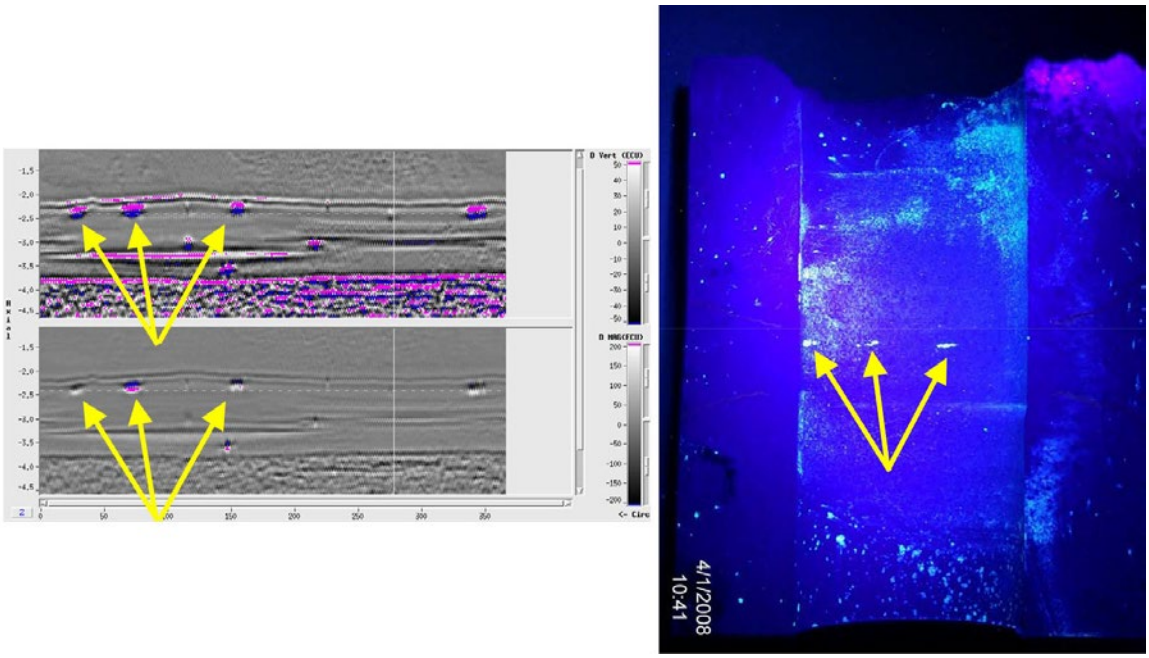

Figure 2.5. ET and PT Results from a Retired Pressurizer DMW in a Safety Relief Nozzle (Weakland 2008). PT and subsequent DT confirmed surface-connected hot tears ranging from 5.6 to 9.65 mm (0.22 to 0.38 in.).

2.5.6 Summary of Field Results

Although ET is not required to be used for Code inspections of DMWs and J-groove welds, it actually has been used extensively both domestically and abroad. There is a relatively small population of flaws detected by ET that have other confirmatory data (PT or DT). However, the available data are very positive for demonstrating the validity of the technique for this application.

The available field data indicate that a minimum detectable length of 3–4 mm (0.12–0.16 in.) is achievable in a practical fashion. Because N-770-2 notes an acceptance criteria of 1/16-inch for surface flaw length (see Note 15.d and 17 in the Code Case), this minimum detectable length of 3–4 mm (0.12–0.16 in.) is approximately twice what is defined in the Code Case. Thus, if one were to only consider field results, it would appear that current minimum ET detection lengths would likely not provide enough resolution to meet the criteria provided in CC N-770-2.

Regarding minimum flaw depth, this is expected to be less than 0.25 mm (0.01 in.), primarily based on steam generator tube ET history.

3.0 Motivation for this Work

Using a “trust, but verify” approach to industry claims on the effectiveness of peening to mitigate against PWSCC in various forms of high nickel alloys, a number of conditions were considered. Primary among these considerations were:

- Were there any pre-existing surface or subsurface flaws that could challenge the peening effectiveness?
- Could a technique be implemented to confirm that the peening process covered the entire susceptible material?

In the 1980s, there was an extensive program to peen the ID of steam generator tubes to mitigate against PWSCC. In general, the results were less positive for units that were peened that had already been in service than for plants that were peened prior to operation. Although there was no detailed evaluation program, it was widely assumed that plants already in service had pre-existing flaws that were deeper than the peening depth (approximately 0.08 mm [0.003 in.]), which when peening would put the crack tip in a higher tensile stress. Similarly, an earlier mitigation process for pipe and safe-end welds, mechanical stress improvement process (MSIP), had a regulatory-imposed limit of pre-existing flaws that had to be less than 30% through-wall, based on this same consideration of not allowing a pre-existing flaw with a depth greater than the mitigation depth (MSIP compressive stresses extend to approximately 50% through-wall).

Additionally, there have been two instances of leaking bottom-mounted instrumentation nozzles’ J-groove welds (South Texas Project and Palo Verde) that were attributed to pre-existing subsurface voids/inclusions at the toe of the weld adjacent to the penetration nozzle (Thomas 2003; Berles 2014). Thermal/mechanical stresses during operation were attributed with eventually rupturing the thin ligament (<1.02 mm [0.04 in.]) and exposing the susceptible region to primary water. It is conceivable that a peening process could potentially break such a thin ligament, if one existed.

There are two primary concerns expressed by industry about using ET for J-groove welds. One is false positives and the other is coverage of the complex geometry, especially at the toe of the weld with a steep side “hill” geometry (EPRI 2016). In the industry response to a Request for Additional Information on MRP-335, false positives were cited as a concern.

Even with the existing ET technology for inspecting high nickel-alloy welds, there is an additional limitation of coverage because of geometric constraints at the toe of the weld. The physical size of the ET coils and the acute angle between the CRDM nozzle and reactor vessel head creates an interference near the toe of the weld. To address the geometric limitations, PNNL evaluated an alternate coil design using a flexible probe that had been developed for other challenging geometries for aerospace and turbine inspections.

Accordingly, the PNNL program addressed the following aspects for ET capabilities for J-groove welds and DMW butt welds as a pre-peening condition assessment:

- detection limits for length and depth so that the assumptions used in the analysis are satisfied
- subsurface flaw detection to address the field experience from two operating plants
- a review of false positive calls comparing ET and PT
- inspection coverage limitations and improvements because of geometric limitations with J-groove welds
- qualitative residual stress measurements.

4.0 Assessment of Eddy Current Examination Detection Capability (Laboratory Evaluation)

4.1 Eddy Current Probes Used in this Study

A variety of probes were used for ET assessments of components in this study (Table 4.1). Each probe used in this study was selected for a combination of performance specifications, sensitivity to flaws of a certain size and orientation, and form factor for accessing remote inspection regions (i.e., uphill portion of CRDM nozzle penetration region). Probes used throughout this study are shown in Figure 4.1 through Figure 4.3.

Table 4.1. Summary of Eddy Current Probes

Probe	Model	Type	Excitation Frequency Range (MHz)
UniWest Flex Coil	FET-3427	Cross-wound coil in circumferential direction on flexible probe body for improved surface compliance near J-groove weld	0.2–2.0
UniWest Flex Coil	FET-3268	Cross-wound coil in helical direction on flexible probe body for improved surface compliance near J-groove weld	0.2–2.0
WesDyne “Grooveman”		+ Point probe on articulating body for improved compliance with examination surface	0.2–0.4

Figure 4.1. Flex Probes with Coils Wound in Helical Direction

Figure 4.2. Flex Probe with Coils Wound in the Circumferential Direction

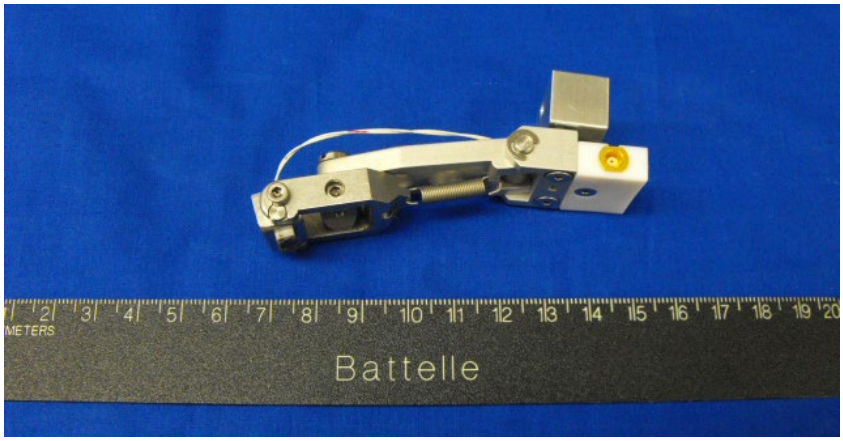

Figure 4.3. WesDyne Grooveman Probe with Articulating Body

4.2 Eddy Current Data Acquisition and Scanning Systems Used in this Study

4.2.1 Eddy Current Examination Setup

A four-axis scanner was used to acquire data throughout this study. The scanner is capable of encoded motion in X, Y, Z, and θ directions. Motion in the X, Y, and Z directions is achieved with three linear rails, and motion in the θ axis is achieved by a rotation table mounted to a hydraulic scissor lift at the bottom of the scanner structure. This configuration was used primarily for examination of the CRDM specimens as shown in Figure 4.4 where the CRDM nozzle is mounted to the rotation table and rotated to provide indexing for fillet weld examinations.

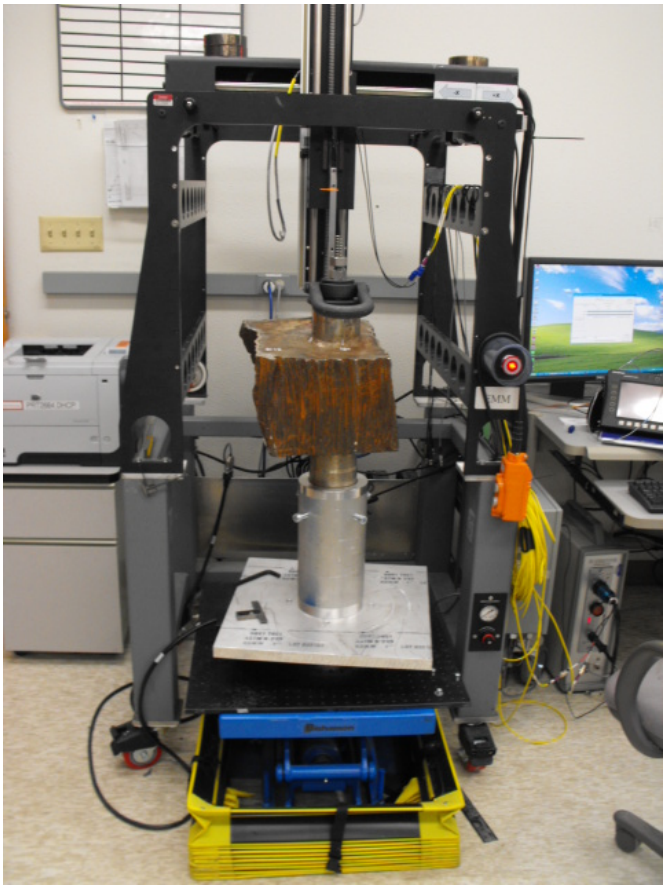

Figure 4.4. Translation Stage Capable of Motion in Four Axes (X, Y, Z, rotation) Used for Examining Specimens in this Study

A removable table surface was mounted to the scanner for acquiring X-Y data of flat specimens as shown in Figure 4.5. The translation stage was controlled by a Windows PC using custom motion control software. A pulse-on position scheme was used where the controlling PC triggered the data acquisition equipment at each measurement location. For this study, the data acquisition equipment consisted of a WesDyne IntraSpect eddy current system, which was controlled by another Windows PC. The data acquisition hardware is shown in Figure 4.6.

The mechanical accuracy of the examination system is determined by the pitch of the linear rail screw and the number of motor pulses per revolution of the motor. For the examination system used in this study, the mechanical accuracy of the system was significantly smaller than the scan and index steps used for these examinations; that is to say, the examinations presented in this report were not acquired near the accuracy and repeatability limit of the examination system. In the eddy current acquisition and analysis software, a pixel of data has a width representing one scan increment and a length representing an index increment. For example, if the scan step size is 0.254 mm (0.010 in.) and the index step is 0.5 mm (0.020 in.), then a pixel of data in the software will represent a 0.254 mm $\times$ 0.5 mm (0.010 in. $\times$ 0.020 in.) area. Sizing of responses during analysis is accomplished by using cursors to measure distances within the examination region and, with the positional information provided in analysis software, the cursor positions are given directly as absolute position. Length sizing of responses, such as notches, is then accomplished by placing the sizing cursors over the relevant flaw response pixels, as determined by the analyst's procedure, and directly reading the cursor position.

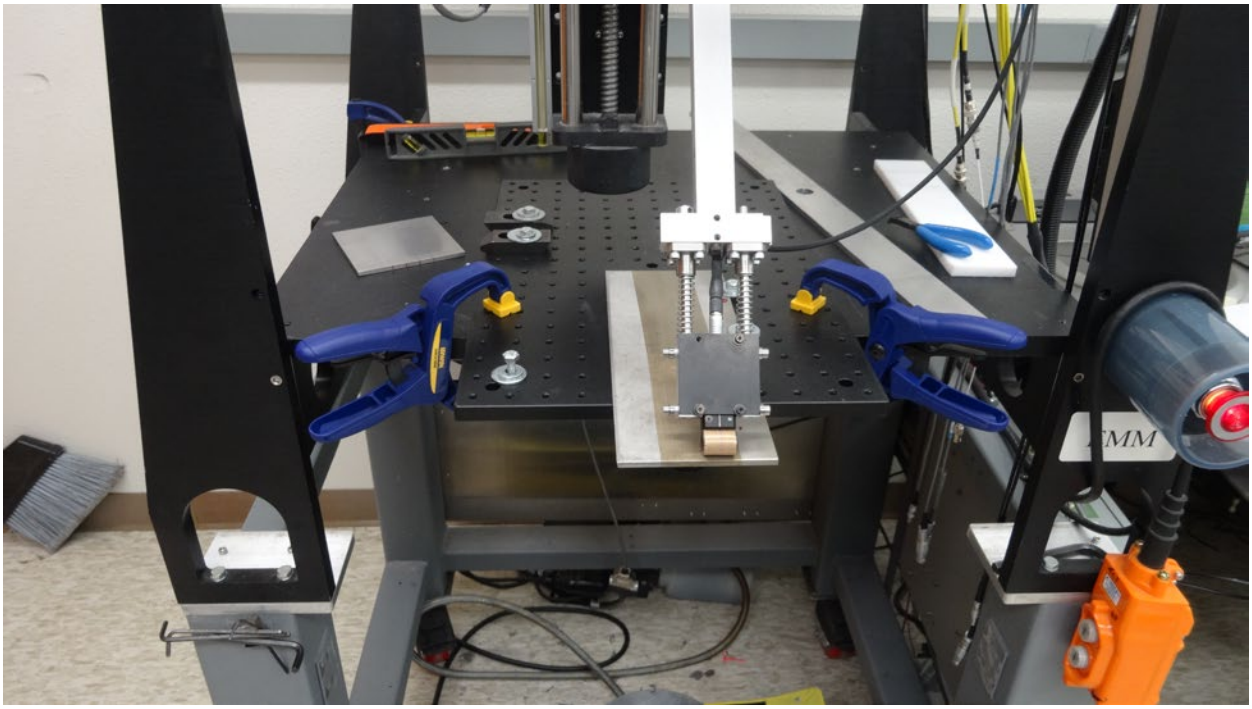

Figure 4.5. Translation Stage with Table Insert for Acquiring Data on Flat Specimens

Figure 4.6. WesDyne IntraSpect Eddy Current Examination System

CRDM nozzle examinations were conducted in a polar format where the scan direction was radially oriented, and the index steps were in a rotational direction (theta direction) around the axis of the nozzle. These examinations were accomplished using a rotation table as shown in Figure 4.5, for effective motion control and precise movement. The radial motion for the scan axis was configured to use a 0.254 mm (0.010 in.) linear step size in a radially inward direction starting on the reactor pressure vessel (RPV) head material and scanning toward the CRDM

nozzle. The index motion was accomplished using a 0.3° index step by rotating the sample. Total scan size varied for each CRDM specimen because of the slope of the RPV head relative to the vertical orientation of the nozzle, creating unique access restrictions in some cases. The full examination of the fillet weld was accomplished by acquiring data in several smaller examinations (to accommodate the non-symmetric nature of the components and preserve scan motion in a radially outward direction), and rotational indexing around the circumference of the CRDM nozzle outer diameter (OD). Depending on the access challenge presented by the RPV tilt, samples were split into several smaller examinations that covered as little as 10° for high-tilt samples and as much as 45° for relatively flat samples that were extracted near the top of the RPV head. The examination region started 6.35 mm (0.25 in.) before the cladding and moved radially inward ending on the J-groove weld. This region can be seen in Figure 4.7 where the edge of the cladding is shown with a black line around the RPV head. The examination area was determined using manual hand scanning with an ET probe and determined the scan limits for subsequent encoded examinations.

Figure 4.7. Photo Showing CRDM Nozzle Examination Region from the Edge of Cladding, Indicated by Black Line, up to the J-groove Weld

Additional examinations including the top edge of the fillet weld were conducted from the CRDM nozzle OD. In these examinations, the WesDyne Grooveman probe was placed on the CRDM nozzle OD and scanned down to the top of the fillet weld. These data sets used the rotation table to index the CRDM specimen. An image of this examination configuration is provided in Figure 4.8. Data was collected in 45° sections using a 0.5 mm (0.020 in.) scan increment in the Z-axis and a 0.5° step in the index axis (θ).

The flat plate samples were examined using a scan increment of 0.25 mm (0.010 in.) and an index step of 0.25 mm (0.010 in.). It is important to note that the resolution of the data can be synthetically decreased through use of the Odd/Even tool in the analysis software, which effectively doubles the index step size by ignoring every other line in the data file. This allows data to be acquired at a fine step size and then evaluated in the analysis using the acquired step size as well as twice the step size (i.e., data can be acquired at 0.5 mm (0.020 in.) step and analyzed at this step or at 1.02 mm (0.040 in.) step using the odd/even option). This is useful for assessing and comparing to a data set using a larger step increment without actually needing to acquire data at the larger step size.

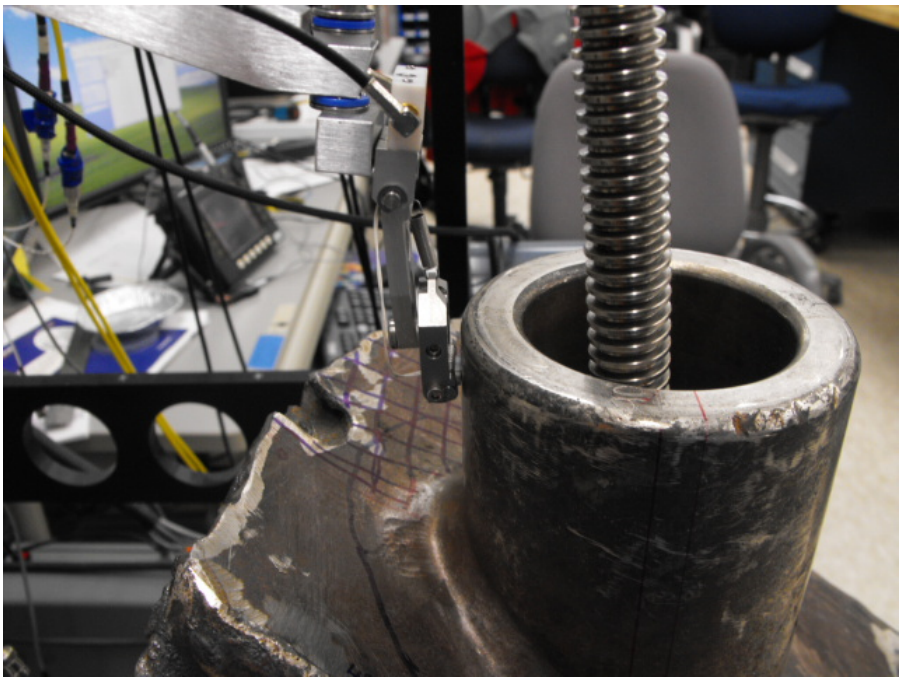

Figure 4.8. CRDM Nozzle OD and Top of Fillet Weld Examination Using WesDyne Probe

4.2.2 Eddy Current Coverage and Limitations

Because of the use of a scanner with primary motion in Cartesian axes and the large tilt of the RPV head material relative to the CRDM nozzles, select portions of the J-groove weld and RPV material were precluded from examinations. An example of a region where no coverage was achieved is provided in Figure 4.9. Examination of these regions requires either manual hand scanning or a specialized scanning apparatus capable of accounting for the tilt of the RPV head and maintaining proper probe compliance with the examination surface.

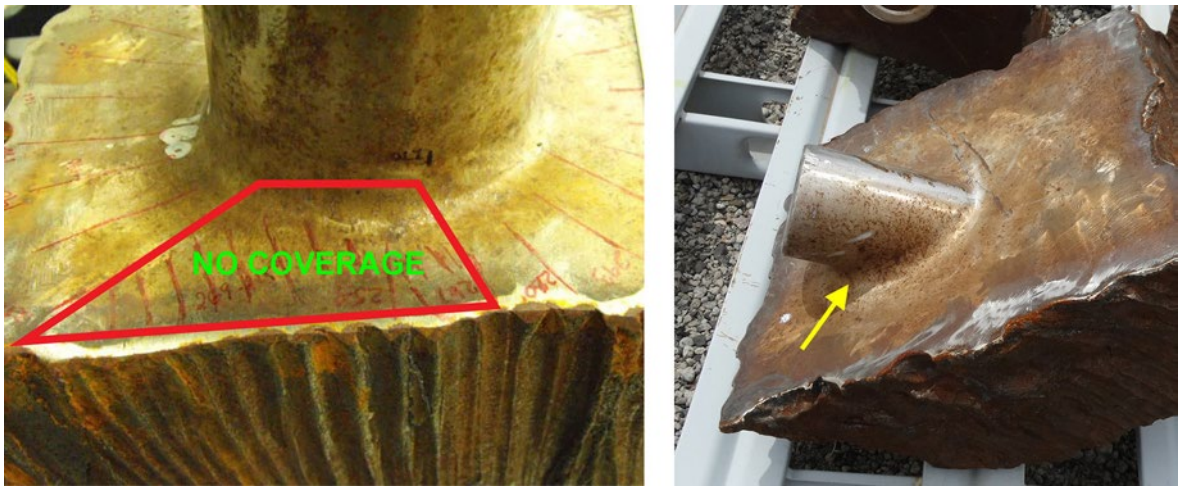

Figure 4.9. Example of Regions with Limited or No Examination Access Due to the Curvature of the Inside Surface of the RPV Head that Occurs Downhill from the Top-Center of the RPV Head

4.3 Materials and Mockups Used in This Study

4.3.1 CRDM Nozzle Specimens

The four CRDM specimens selected for pre-peening ET assessments were also used for assessing access challenges and limitations of common ET probes. These specimens were selected based on the access challenges presented around the J-groove weld caused by the angle between the RPV head and the CRDM nozzle. Limited data were acquired on CRDM Specimen #3 as it was included in an initial assessment for determining which samples would be used for this study, but it was eliminated midway through the pre-peening NDE effort. Detailed dimensional analyses and individual coordinate systems for each of the remaining three specimens were conducted.

Figure 4.10 is a diagram of a CRDM penetration-nozzle assembly with a section of the RPV head, the penetration tube, and the J-groove weld, which is the focus for weld residual stress in these components. Most of the interface between the RPV head and the penetration tube is an interference fit and is not watertight. The only barriers between the primary coolant and outside containment are the J-groove weld, buttering, and the penetration tube below the weld on the wetted side.

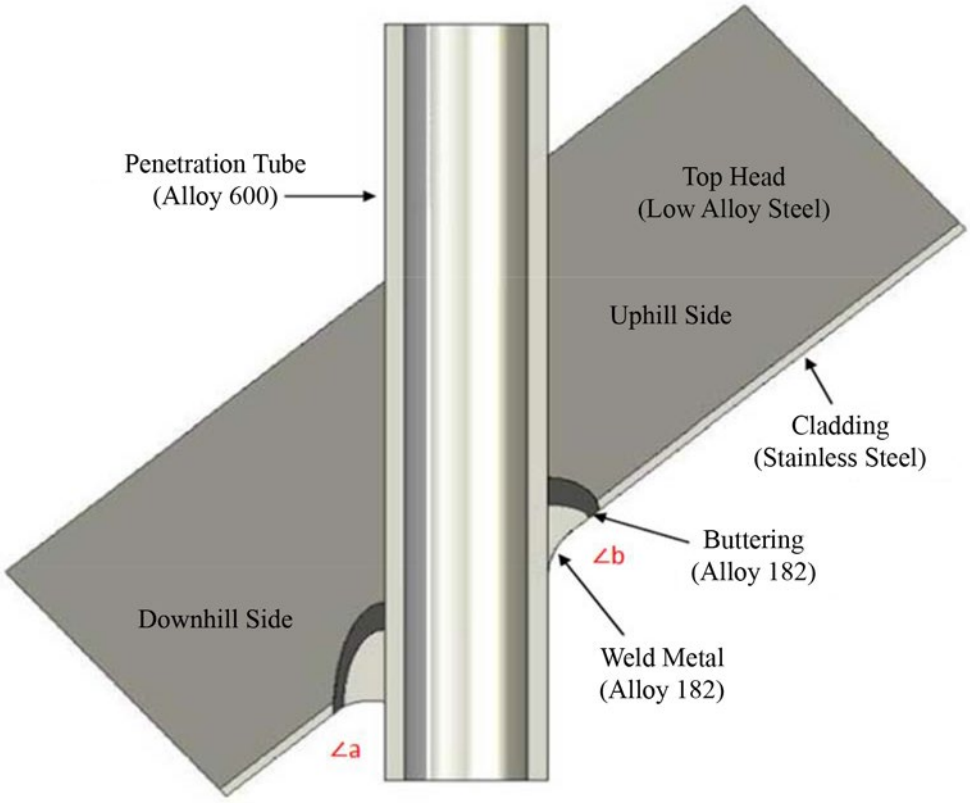

Figure 4.10. Control Rod Drive Mechanism Penetration-Nozzle Assembly

As mentioned above, the area of focus for these mockups is the area of the J-groove welds and the immediate parent material adjacent to the welds. In Figure 4.10, these are labeled as ∠a and ∠b. In Table 4.2, these angles are highlighted in yellow. The angles corresponding to the requirements for the three different CRDM penetration-nozzle assemblies as defined in the project statement of work (SOW) are computed by subtracting the ∠a values from 90°. Therefore, the "downhill" angle into the RPV head for CRDM penetration nozzle #6 is 31.3°. For CRDM penetration nozzle #9, the angle is 19.3°, and for CRDM penetration nozzle #12, the angle is 9.2°. PNNL characterized multiple CRDM penetration-nozzle assemblies; however, the green highlighted mockups are the mockups that have been identified in the modified SOW for this project and were targeted as the specific mockups of interest for NDE, weld residual stress, and peening activities on this project. Thus, CRDM mockup specimen #6 has the highest degree of incidence from the normal (of the RPV head) and is therefore located well off the top-dead-center of the RPV head, so the penetration tube is inserted towards the side of the RPV head. CRDM mockup specimen #9 was located in the mid-range between the top and side of the RPV head. CRDM #12 was located near the top of the RPV head.

4.3.1.1 CRDM Penetration-Nozzle Assembly Coordinate System

For consistent measurements and testing, a coordinate system was generated and physically marked (etched) on each CRDM penetration-nozzle assembly mockup. This consists of a 0° mark at the lowest absolute angle on the wetted side of the mockup. In other words, the 0° mark is at the ∠a of the CRDM mockup on the "downhill" side. From the zero point, the coordinate system increases in angle in the counter-clockwise direction, with marks at 90°, 180° (at the ∠b location), and 270°. Figure 4.11 illustrates the azimuthal coordinate system on these mockups.

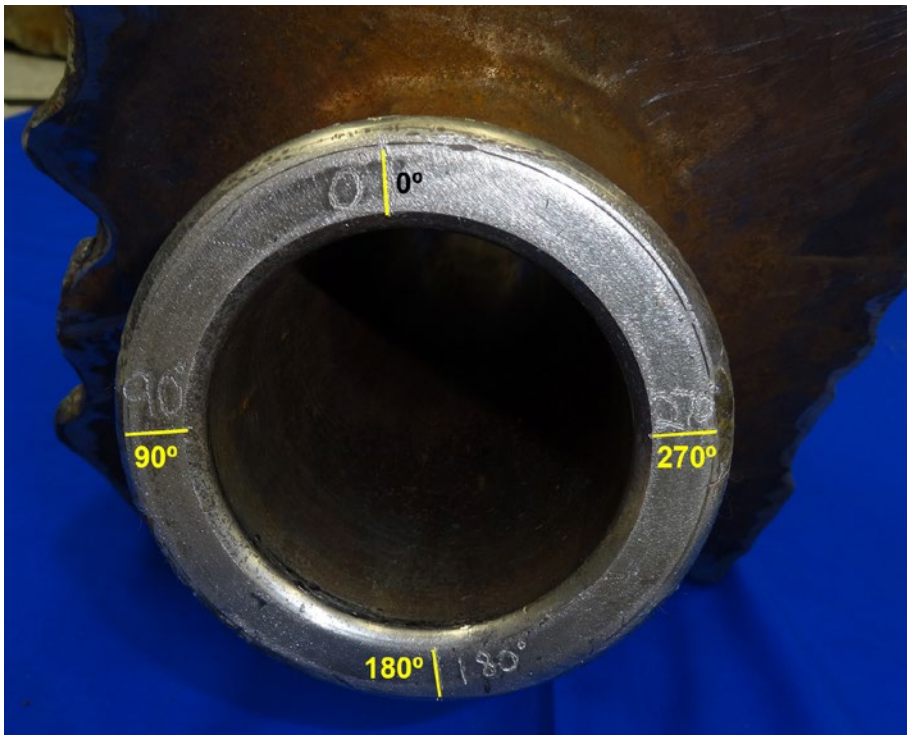

Figure 4.11. View of Azimuthal Coordinate System of Inside Surface of the RPV Head ("wetted" side) for a CRDM Penetration-Nozzle Assembly Mockup

Table 4.2. Physical and Dimensional Data for All CRDM Penetration-Nozzle Assembly Mockups Identified for Potential Use in This Study with the Exception of CRDM #5 and #10

	CRDM Penetration-Nozzle Assembly Measurements															RPV Head Cut-Out Measurements			Total Specimen
	Inside Surface of RPV Head "Wetted Side"								Outside Surface of RPV Head										
Mockup Number	Top Angle ∠b	Bottom Angle ∠a	90° - ∠a	Top Length (mm)	Bottom Length (mm)	ID (mm)	OD (mm)	Wall Thickness (mm)	Top Angle	Bottom Angle	Top Length (mm)	Bottom Length (mm)	ID (mm)	OD (mm)	Wall Thickness (mm)	X-Axis (mm)	Y-Axis (mm)	Z-Axis (mm)	Weight (kg)
CRDM #3	131.1°	43.8°	46.2°	157	38	69	102	16.5	51.8°	128.2°	258	340	69	105	18	300	313	198	181.3
CRDM #4	120.6°	59.4°	30.6°	163	66	69	102	16.5	56.7°	123.3°	265	337	69	105	18	356	318	203	140.6
CRDM #6	121.3°	58.7°	31.3°	157	69	69	102	16.5	56.2°	123.8°	277	335	69	105	18	284	269	203	136.1
CRDM #7	131.1°	48.9°	41.1°	157	71	69	102	16.5	55.4°	124.6°	366	305	69	105	18	320	305	198	174.6
CRDM #9	109.3°	70.7°	19.3°	140	107	69	102	16.5	73.0°	107.0°	277	244	69	105	18	290	328	198	154.2
CRDM #12	99.2°	80.8°	9.2°	72	58	69	102	16.5	86.4°	93.6°	295	283	69	105	18	271	285	195	127

4.3.2 Calibration Plates

Calibration plates with multiple EDM notches were fabricated for assessing sizing capabilities of ET probes. These two plates were fabricated in stainless steel (SS) and Inconel 600 with the same surface notches in each. A post-fabrication optical assessment was conducted to verify the notch depths were within design specifications. Figure 4.12 provides an overview of the calibration plate design as well as the as-designed size information for each EDM notch. Figure 4.13 shows an example output of the optical profilometer measurement used to measure notch depth. A manual caliper measurement was used to measure the notch lengths and feeler gauges were used to estimate the notch width. A summary of these measurements is provided in Table 4.3. The notches in the Inconel 600 plate were used as reference defects for the work presented in this report.

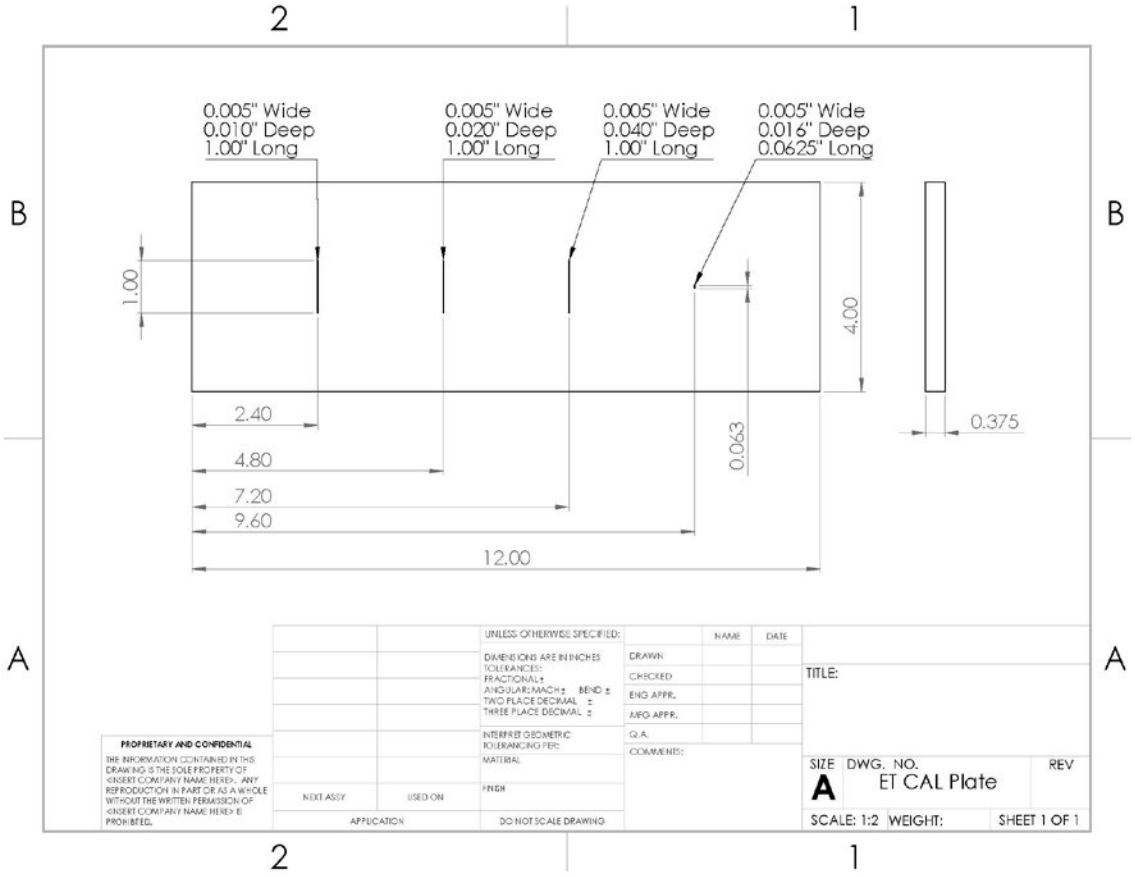

Figure 4.12. Design Drawing of EDM Notches Fabricated in a SS Calibration Plate and an Inconel 600 Calibration Plate

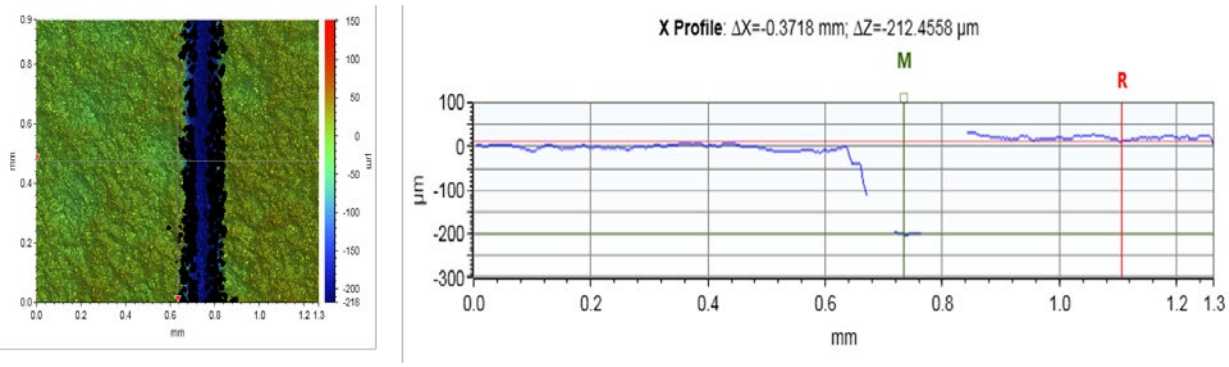

Figure 4.13. Optical Notch Measurement Results Used for True-state Depth Sizing

Table 4.3. Summary of True-state Measurements for SS and Inconel Calibration Plates

Material	Notch Dimensions in inches (Length × Width × Depth), mm (in.)	Measured Length,[a] mm (in.)	Measured Width,[b] mm (in.)	Measured Depth,[c] mm (in.)
SS	25.4 × 0.13 × 0.25 (1.00 × 0.005 × 0.010)	25±0.13 (0.985±0.005)	0.15 (0.006)	0.20 (0.008)
SS	25.4 ×0.13 × 0.5 (1.00 × 0.005 × 0.020)	25.3±0.18 (0.996±0.007)	0.18 (0.007)	0.43 (0.017)
SS	25.4 × 0.13 × 1.02 (1.00 × 0.005 × 0.040)	25.43±0.23 (1.001±0.009)	0.18 (0.007)	0.94 (0.037)
SS	1.6 × 0.13 × 0.4 (0.0625 × 0.005 × 0.016)	1.70±0.13 (0.067±0.005)	0.23 (0.009)	0.36[d] (0.014)
Inconel	25.4 × 0.13 × 0.25 (1.00 × 0.005 × 0.010)	25.45±0.15 (1.002±0.006)	0.15 (0.006)	0.15 (0.006)
Inconel	25.4 × 0.13 × 0.5 (1.00 × 0.005 × 0.020)	25.65±0.23 (1.010±0.009)	0.18 (0.007)	0.04 (0.0017)
Inconel	25.4 × 0.13 × 1.02 (1.00 × 0.005 × 0.040)	25.35±0.13 (0.998±0.005)	0.2 (0.008)	0.91 (0.036)
Inconel	1.6 × 0.13 × 0.4 (0.0625 × 0.005 × 0.016)	1.68±0.08 (0.066±0.003)	0.25 (0.010)	0.36[d] (0.014)

(a) Length was measured using the average of five manual caliper measurements.
(b) Notch width was determined using the average of ten feeler gauge measurements.
(c) Depth measurements were acquired using the optical technique reported earlier. The measured depth represents the average of five depth measurements spread over the length of the notch.
(d) Only three measurements were used for the average due to the short length of the notch.

4.3.3 Stainless Steel Plates with Copper Reflector Strips

Copper strips were adhered to a SS plate to simulate flaw responses. These strips were covered with transparent Teflon tape to prevent the strips from being loosened during examination as shown in Figure 4.14. Two strips were 9.53 mm (0.375 in.) long and 0.25 mm (0.01 in.) wide and another set was 12.7 mm (0.50 in.) long and 0.25 mm (0.01 in.) wide. As

shown in Figure 4.14, one of each size strip was placed in an axial direction and the remaining strips were configured in a circumferential direction.

The intent of this effort was to simulate the 0.5 mm (0.020 in.) deep reference notch in the Inconel 600 calibration plate using narrow copper strips with an adhesion backing for placement on an examination surface. Once the copper strip response was representative of the 0.5 mm (0.020 in.) wide notch, it could be placed on a CRDM nozzle specimen weld in any orientation to further assess detection capabilities in the J-groove weld region.

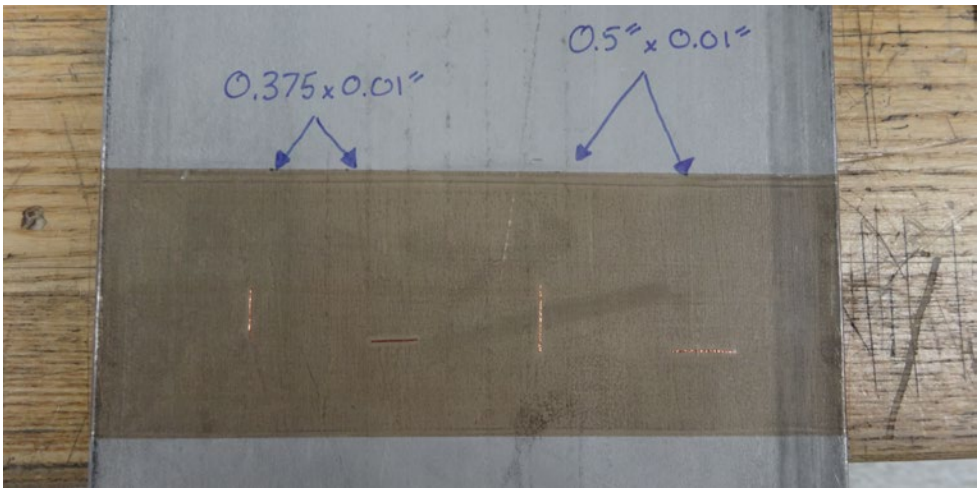

Figure 4.14. Copper Strips were Adhered to a Stainless Steel Plate and Covered with Teflon Tape to Produce Notch-like ET Responses

4.3.4 Bottom-Drilled Hole Standard

For further assessment of subsurface reflectors, a plate was fabricated with a series of bottom-drilled holes of varying diameters and depths. Varying the hole depths results in varied ligament length between the bottom of the hole and the opposite surface. This back-side surface was used for scanning to assess subsurface flaw detection capabilities of eddy current probes. A design drawing of this plate is provided in Figure 4.15 with the true-state remaining ligaments indicated.

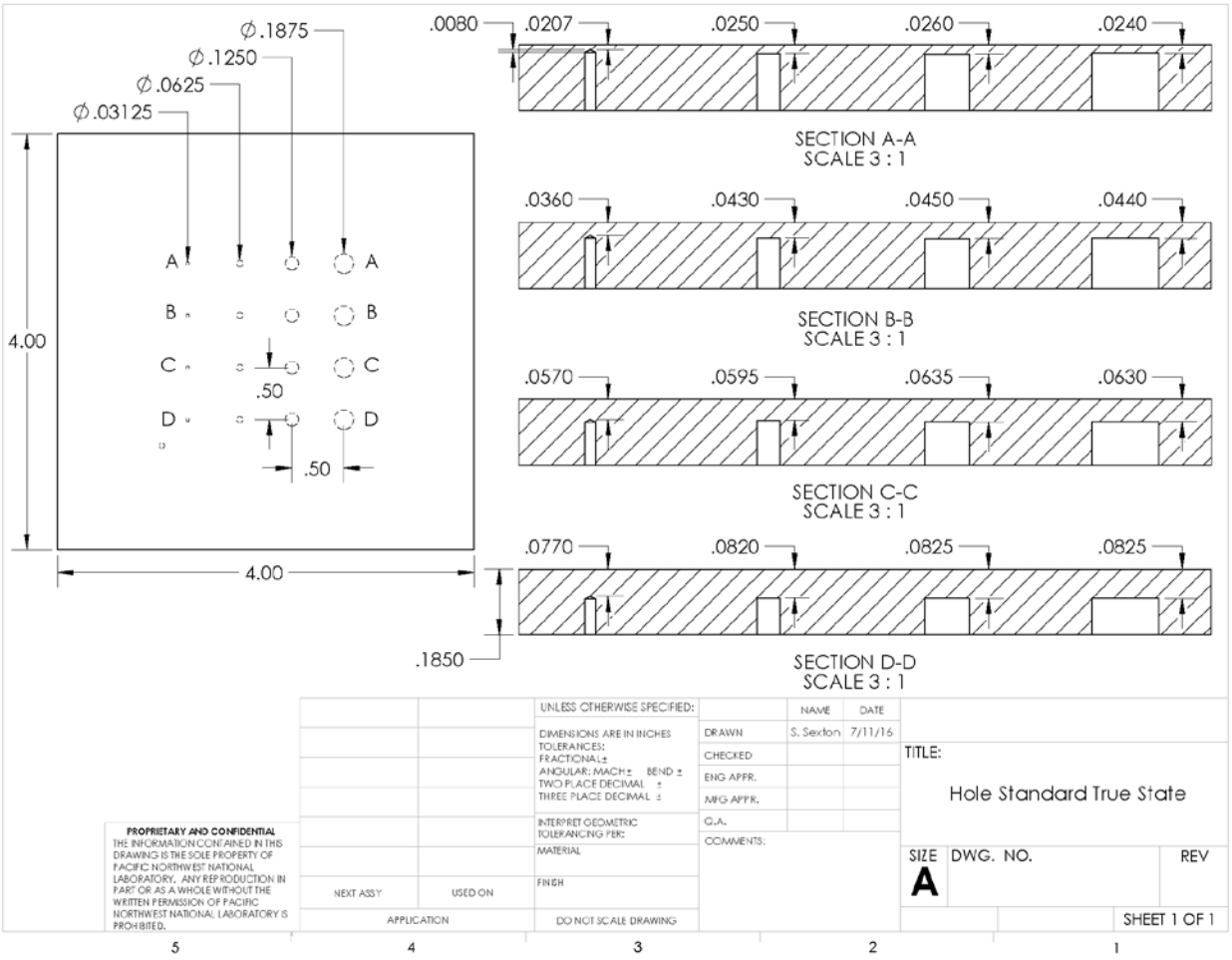

Figure 4.15. Design Drawing of the Bottom-Drilled Hole Plate with As-built Dimensions Showing Remaining Ligament

4.3.5 Cold Spray Plate for Subsurface Flaw Assessments

For assessments of subsurface flaws, a SS plate was fabricated with two machined notches from the back side such that a small ligament remained between the inspection surface and the top of the notches as shown in Figure 4.16. An Inconel cold spray (CS) surface was then sprayed over the inspection surface such that four different depths of material were placed over the notches. The as-sprayed surface is shown in Figure 4.17. Lastly, the CS surface was machined smooth to reduce surface variability for ET examinations. The machined surface can be seen later in Figures 5.11 and 5.12. After machining, the CS surfaces were measured to be 0.13, 0.25, 0.5, and 102 mm (0.005, 0.010, 0.020, and 0.040 in.) thick.

The larger notch cracked during the CS application process, resulting in the crack connecting the subsurface notch to the inspection surface. The smaller notch did not crack during the fabrication process, leaving a single linear subsurface flaw for examination through four different CS thicknesses.

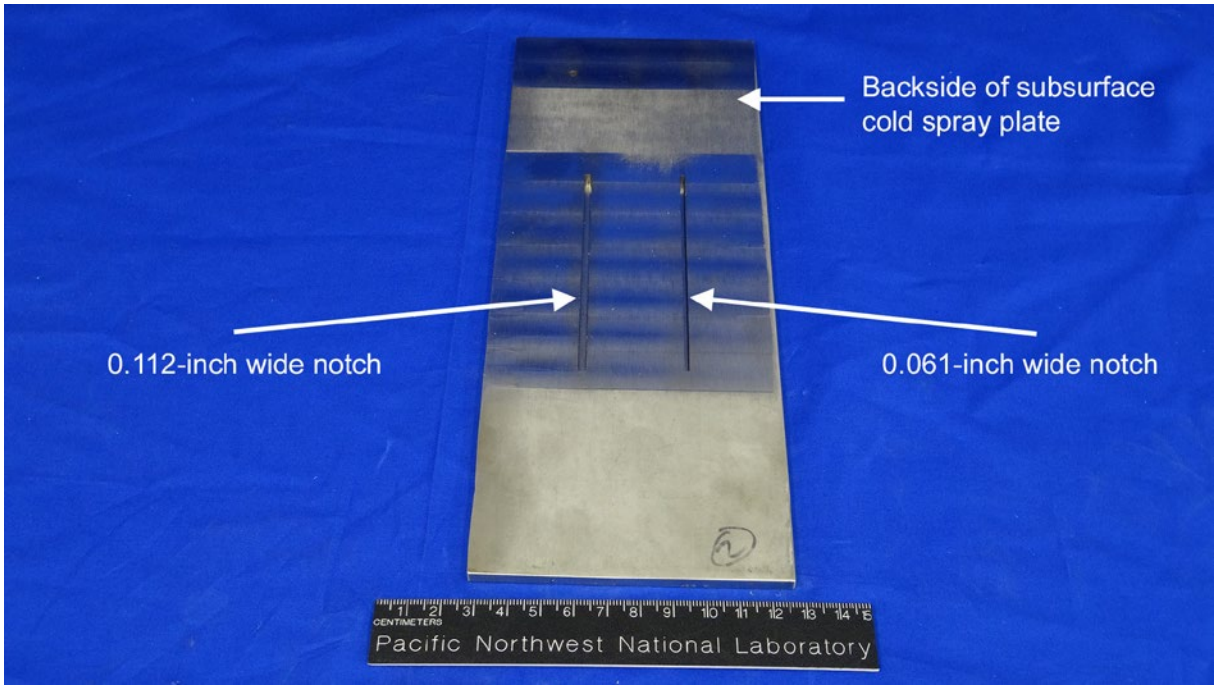

Figure 4.16. Stainless Steel Subsurface Flaw Plate with Two Machined Notches from the Backside to Represent Subsurface Flaws. Inconel cold spray was applied to the front surface resulting in one of the notches breaking through to the front surface.

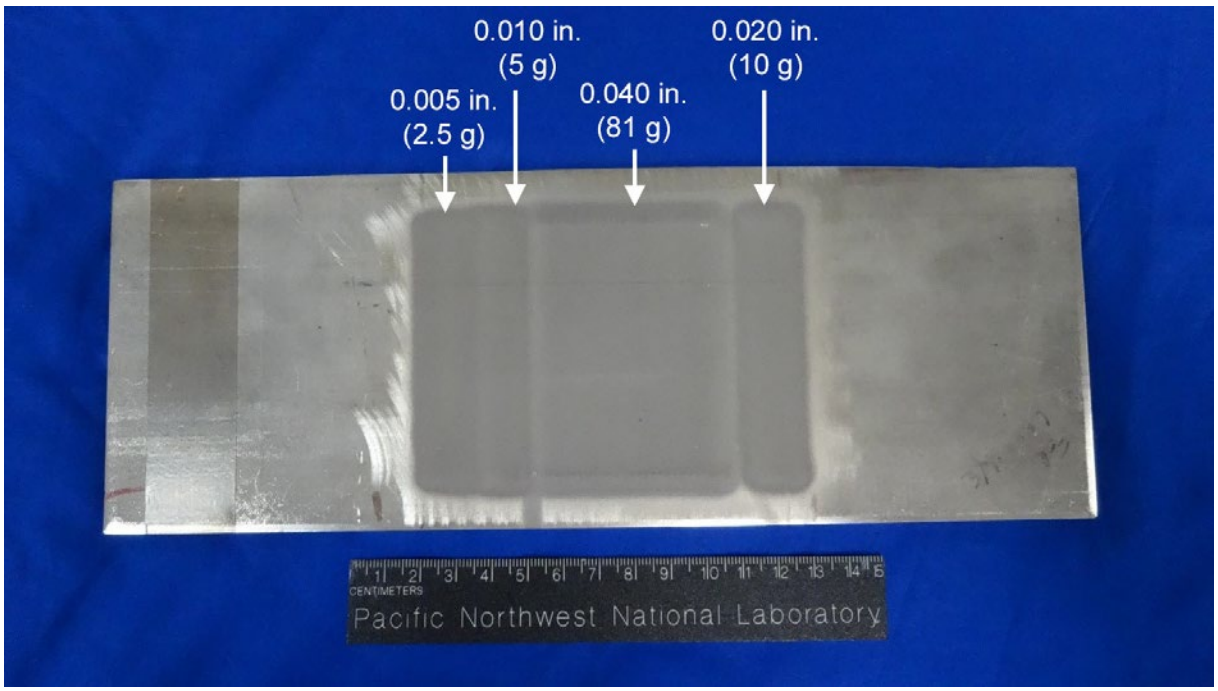

Figure 4.17. Stainless Steel Subsurface Flaw Plate Top Side with Four Different Inconel Cold Spray Layer Thicknesses. The thickness of each layer is given along with the amount of cold spray applied to the surface during fabrication.

5.0 Laboratory-Acquired Data and Results

5.1 Calibration Plate Adhering to ASME Code Section XI Requirements

The four EDM notches in the Inconel 600 calibration plate were used to provide a calibration reference that satisfied ASME Code Section XI requirements. Specifically, the 0.5 mm (0.020 in.) deep notch was used as the reference notch to ensure the signal-to-noise ratio was adequate and to compare responses across multiple examinations.

The calibration scan of the Inconel 600 plate with the Grooveman probe ensured that the system had adequate sensitivity. A magnitude plot of the calibration plate response at 400 kHz is provided in Figure 5.1. The magnitude plot is in the same orientation as the design drawing provided earlier in Figure 4.12 where the notches from left to right have depths of 0.25 mm (0.010 in.), 0.5 mm (0.020 in.), 1.02 mm (0.040 in.), and 0.41 mm (0.016 in.). In this figure, the cursors are placed on the peak response of the 0.5 mm (0.020 in.) deep notch, the amplitude window is set to match the maximum response of the 0.5 mm (0.020 in.) notch, and responses greater than the threshold are colored pink. The 0.5 mm (0.020 in.) deep notch had a maximum response of 86 eddy current units (ECU). Eddy current units are used in the WesDyne analysis software in reference to signal amplitudes. A signal response in ECU is, by itself, a relative quantity, and is only useful when compared to a known response such as a notch or in reference to background noise. A representative sampling of the background noise was measured to have a mean response of 28 ECU, ensuring the signal-to-noise ratio of the acquired data met ASME requirements.

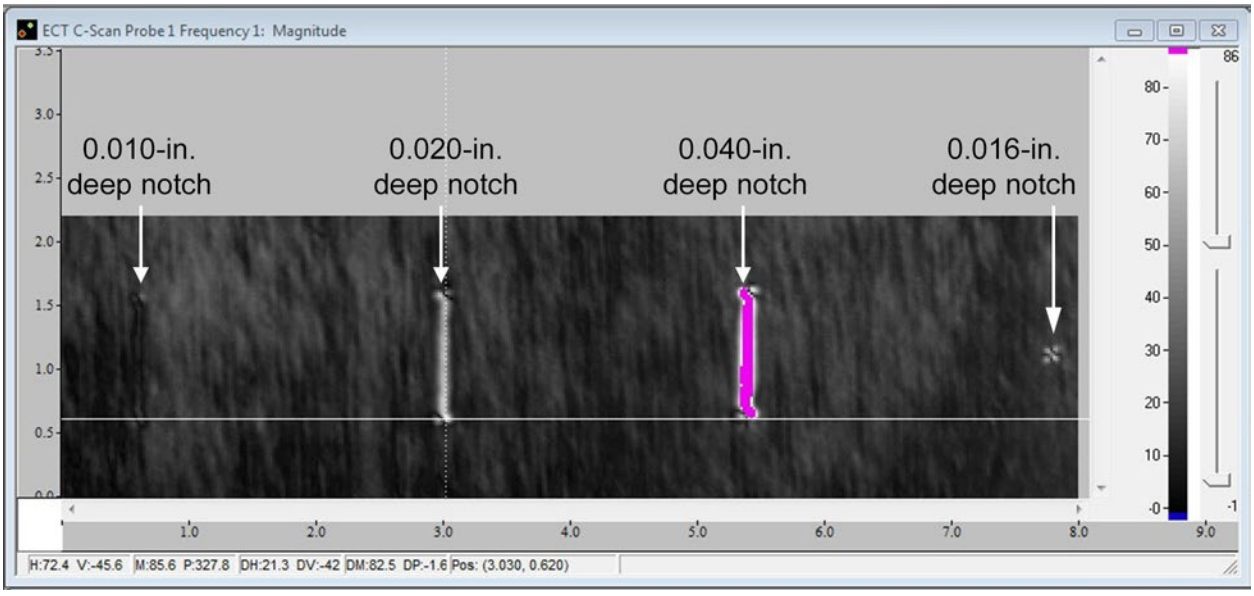

Figure 5.1. Magnitude ET Response of the Inconel 600 Calibration Plate Collected at 400 kHz

The UniWest FET-3268 flex probe, with the helical coil, was also used to acquire ET data on the Inconel 600 calibration plate using probe excitation frequencies of 700 and 350 kHz. The 700 kHz data is provided in Figure 5.2. The 0.5 mm (0.020 in.) deep notch in the calibration plate produced a maximum response of 43 ECU. In this figure, the color bar is set to have a

maximum matching the peak response of the 0.5 mm (0.020 in.) notch, which is indicated with the cursors in the image.

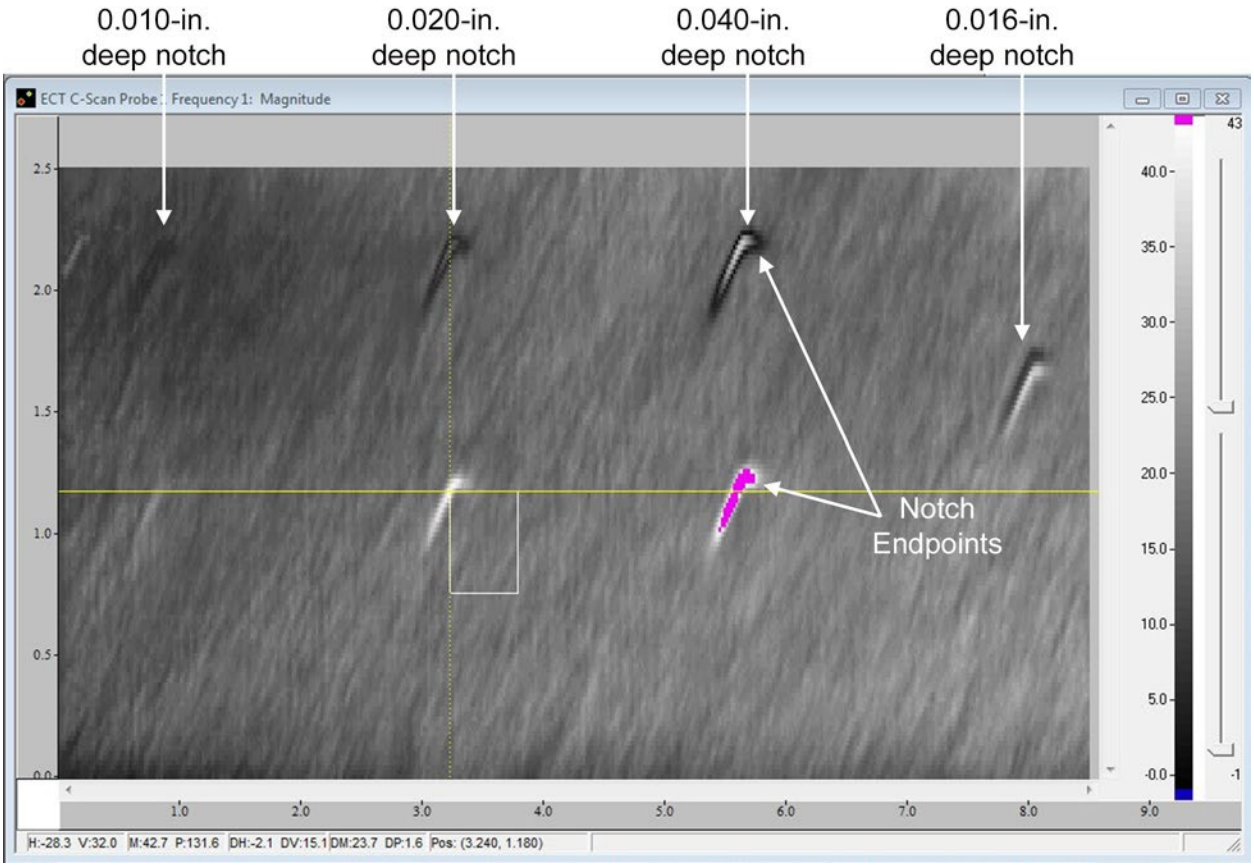

Figure 5.2. Magnitude ET Response of the Inconel 600 Calibration Plate Collected at 700 kHz Using the Flex Probe

Again, as in Figure 5.1, the ET response amplitude threshold is set to match the maximum response of the 0.5 mm (0.020 in.) notch, and responses greater than the threshold are colored pink, or essentially saturated. The white box is used to capture the maximum amplitude threshold of the notch as well as an area of blank (unflawed) material whereby background noise levels are computed. As shown in the 700 kHz data, the edges of the notches are the only features that appear in the ET data. This is caused by the orientation of the coils in the ET probe relative to the notch orientation. The responses from the notch endpoints are tilted at 45° because of the helical orientation of the probe coils. Interpretation of this effect is further analyzed in a subsequent subsection where subsurface notches are covered with CS material and examined with this probe. This artifact was intended to be addressed with an updated probe design of the flex probe (Model FET-3427) where the probe coils are wound circumferentially instead of helically. This optimized probe has yet to be applied to the calibration plates or the CRDM specimens.

5.2 CRDM Penetration J-Groove Welds

Data were acquired on the J-groove weld of CRDM Samples #3, #6, #9, and #12 using the WesDyne Grooveman probe. Additional data were acquired on CRDM #12 using the UniWest FET-3268 flex probe (with the helical coil pattern). Two approaches were used to gain access to

the J-groove fillet weld between the RPV and the CRDM nozzle. The first approach was done from the RPV material with the probe being scanned along the RPV material up onto the J-groove fillet weld as shown in Figure 5.3. This approach resulted in the most coverage of the weld. The second approach was performed from the CRDM nozzle OD with the probe scanning down the nozzle OD and onto the J-groove weld. This approach resulted in significantly less coverage over the weld. A photo of the second examination approach is provided in Figure 5.4.

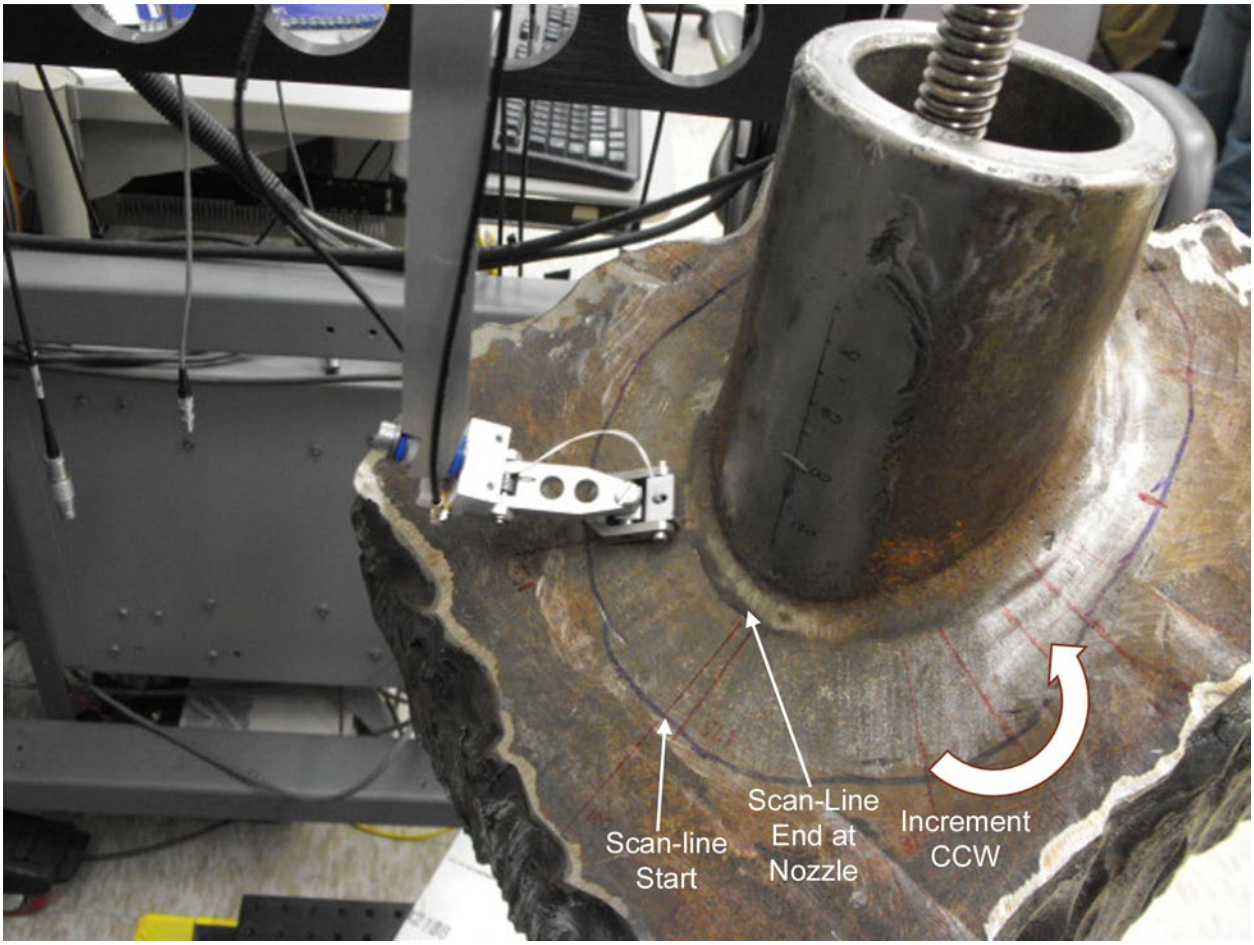

Figure 5.3. CRDM Sample #6 Examination of J-groove Fillet Weld and Portions of RPV Head

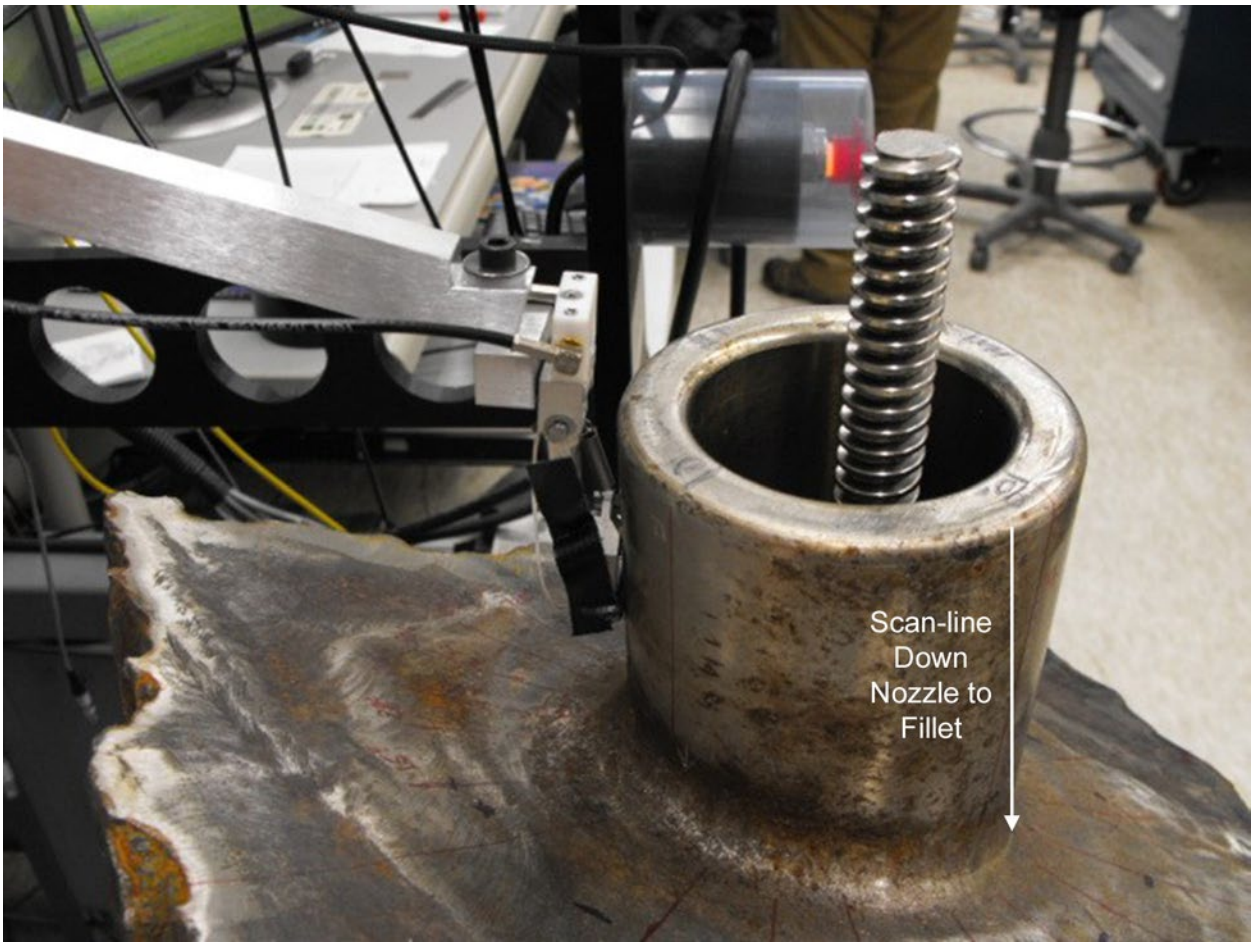

Figure 5.4. CRDM Sample #9 Examination of J-groove Fillet Weld and Portions of the CRDM Nozzle OD

Due to access challenges discussed earlier, the examination of each CRDM was performed in several smaller examinations where the probe fixtures and scanning configuration were optimized for a limited region to ensure proper alignment. A summary of degrees of coverage of each examination performed for each sample with the Grooveman probe is provided in Table 5.1.

Table 5.1. Degrees of Coverage of Each CRDM Sample Grooveman Probe Examination

Sample 3	Sample 6	Sample 9	Sample 12
150–180	90–100	2–23	6–9
180–210	94–115	21–42	5–22
210–225	100–115	40–55	20–35
225–240	113–134	53–74	33–48
237–250	114–142	72–93	46–61
	132–177	91–106	59–74
	135–180	104–125	72–87
	175–220	123–144	85–100
	218–233	142–163	98–113
	231–246	161–182	111–126
	244–259	180–201	124–139
	257–272	199–220	137–152
	270–291	215–230	150–165
		228–243	163–178
		241–256	177–192
		254–269	190–205
		267–282	203–218
		280–295	241–256
		293–309	254–269
		306–321	267–282
		319–334	280–295
		332–347	293–308
		345–360	306–321
			319–334
			332–347
			345–360

Examinations performed on the RPV head material covered a region starting at the edge of the strip cladding and ending on the J-groove weld. This coverage area can be seen in the representative magnitude data in the top of Figure 5.5. In this figure, the strip cladding response is shown in the magnitude data as a vertical response on the left of the image and the J-groove weld response is shown as a vertically oriented response on the right side of the image. Surface roughness on the RPV material, which generically could pose challenges for field applications as the sensitivity of the method is dependent on the surface condition of the weld (Crooker et al. 2014), contributed to a higher background noise level compared to the Inconel calibration block. In this example data set, the mean background noise was observed to be approximately 35 ECUs.

The CRDM samples were not found to contain any crack-like features or subsurface indications. The predominate features of note across all of the data sets were limited to geometric features caused by surface roughness, surface gouges, and weld slag that was never removed during fabrication. An example of the surface gouge is shown in Figure 5.6, which is from the

Sample #6 examination between 132° and 177°. An example of a weld slag response acquired on Sample #9 between 199° and 220° is provided in Figure 5.7.

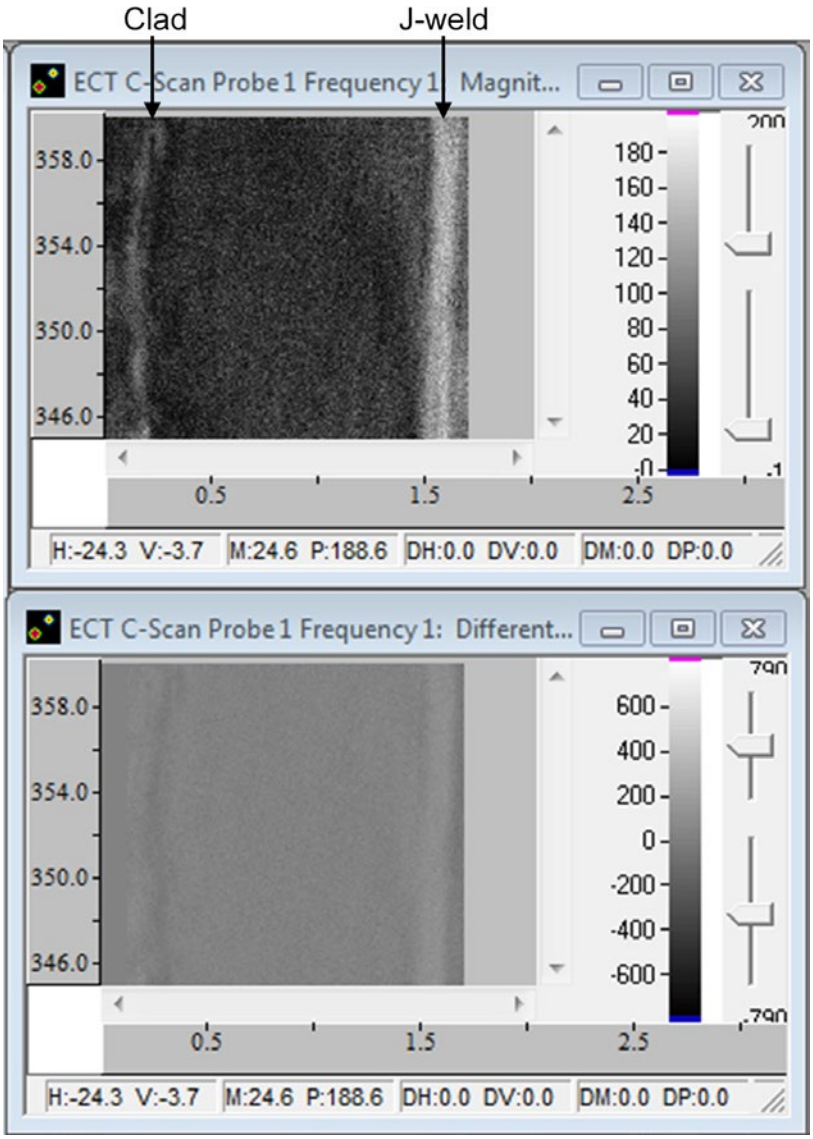

Figure 5.5. Grooveman Probe Examination Data from 345°–360° Using 400 kHz Showing the Magnitude C-scan (*top*) and the Differential Magnitude C-scan (*bottom*). Cladding response is shown at the start of the scan line on the left and the J-groove weld is shown at the end of each scan line on the right.

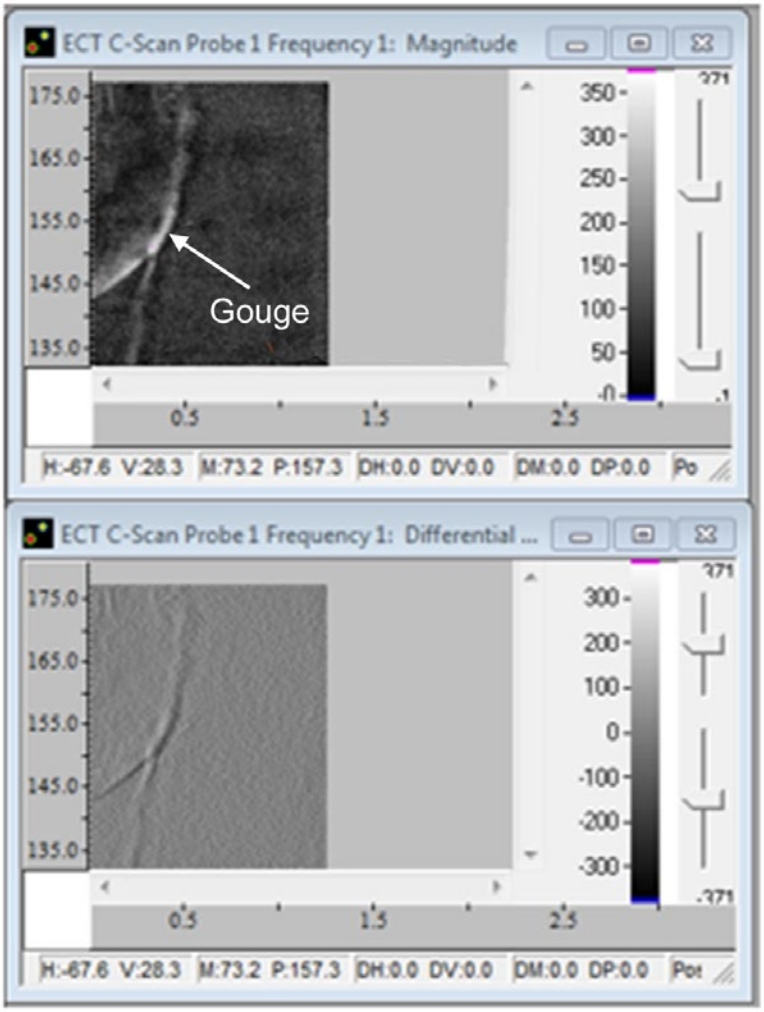

Figure 5.6. Example of Surface Gouge Response from Examination of Sample #6 Between 132° and 177°

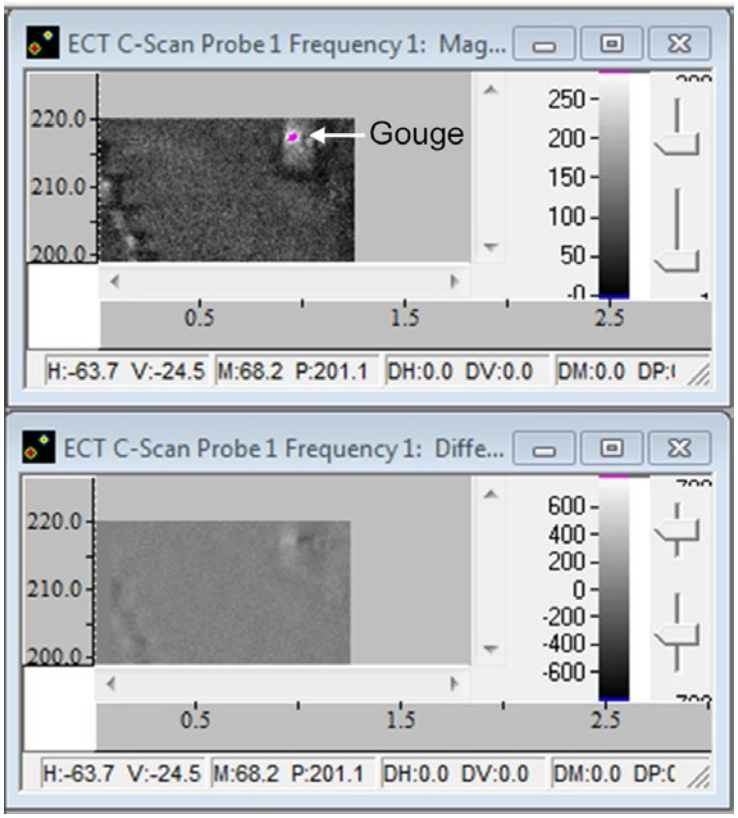

Figure 5.7. Example of Weld Slag Response Shown in Pink on Upper Image of C-scan Magnitude Response from Sample #9 Examination Between 199° and 220°

5.3 Subsurface Flaw Detection Examinations

Actual subsurface flaws are difficult to produce, so PNNL made laboratory simulations of subsurface flaws with flaw sizes based on published reports on subsurface voids/inclusions in failed bottom-mounted nozzle J-groove welds (South Texas Project and Palo Verde, 1.5 mm and 2.54 mm [0.06 in. and 0.1 in. wide], respectively) (Thomas 2003; Berles 2014). Voids were simulated by machining grooves on the back side of a SS plate to within approximately 0.025 mm (0.001 in.) of the surface. The surface was then coated using a process referred to as “cold spray” to provide ligaments ranging from 0.76 mm to 1.5 mm (0.03 in. to 0.06 in.). The coating material was Alloy 625, which is the available powder closest in electrical properties to Alloy 182 weld metal.

5.3.1 Bottom-Drilled Hole Standard

Examinations of the bottom-drilled hole standard were performed using the WesDyne Grooveman probe and the optimized flex probe. The examinations conducted using the Grooveman probe were performed using scan steps of 0.25 mm (0.010 in.) and increment steps of 0.25 mm (0.010 in.). The examinations conducted using the optimized flex probe were performed using a larger scan step of 0.5 mm (0.020 in.) and increment step of 0.5 mm (0.020 in.) because of the larger coil size and overall increased probe footprint. Data were acquired using 400 and 200 kHz operating frequencies for both probe designs. A photo showing an overview of the scanning configuration used with the Grooveman probe is provided in Figure 5.8.

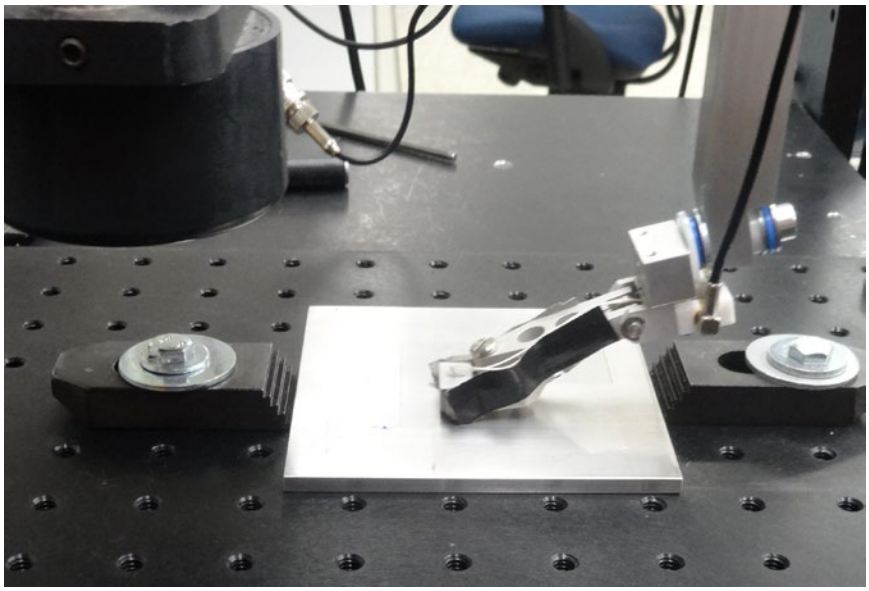

Figure 5.8. Examination of Flat-Bottom Hole Standard using the WesDyne Grooveman Probe

The Grooveman probe performed well when the remaining ligament of holes was small and the diameter was larger as shown in the example magnitude C-scan data set provided in Figure 5.9 and the summary of detection results given in Table 5.2. This probe was able to detect the entire row of shallow holes with the smallest remaining ligament, and it successfully detected three of the four holes in the next row with increased remaining ligament. One challenge with this plate design is the lack of a linear element with each target feature. The small diameter of the holes essentially turns them into point defects, and the lack of a linear characteristic makes them more difficult to detect using ET.

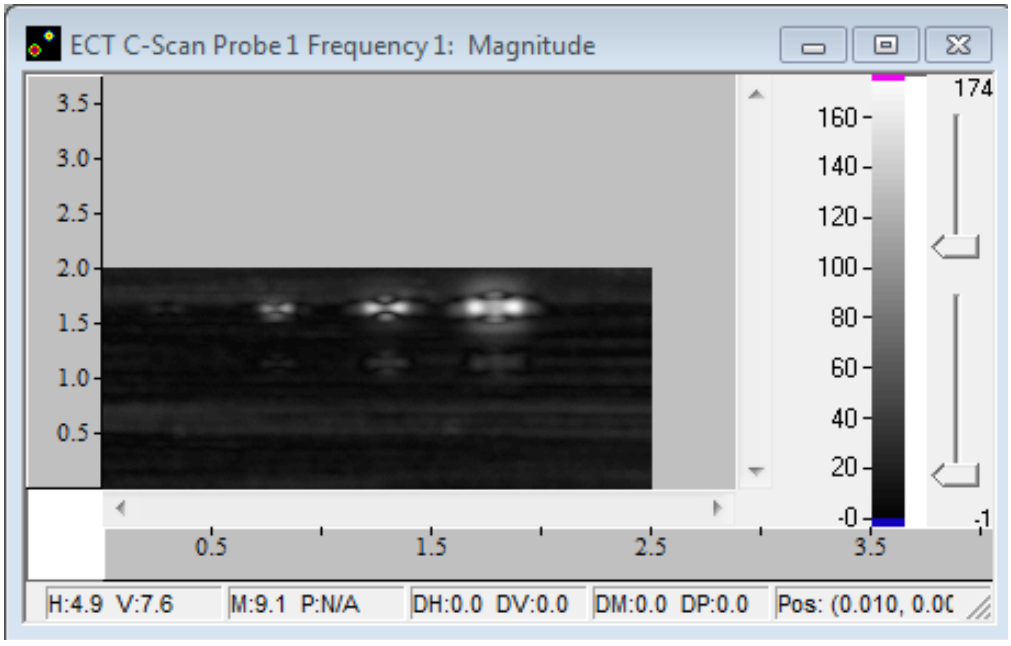

Figure 5.9. C-scan Magnitude Data of the Bottom-Drilled Hole Plate Acquired at 400 kHz Using the Grooveman Probe

Table 5.2. Bottom-Drilled Hole Plate Summary of Detection Results Using Grooveman Probe

Row	Hole Diameter, mm (in.)	Remaining Ligament, mm (in.)	Grooveman Probe, 400 kHz
A	0.79 (0.03125)	0.51 (0.02027)	Detected
A	1.6 (0.0625)	0.64 (0.0250)	Detected
A	3.18 (0.125)	0.66 (0.0260)	Detected
A	4.76 (0.1875)	0.61 (0.0240)	Detected
B	0.79 (0.03125)	0.91 (0.036)	Not Detected
B	1.6 (0.0625)	1.09 (0.043)	Detected
B	3.18 (0.125)	1.14 (0.045)	Detected
B	4.76 (0.1875)	1.12 (0.044)	Detected
C	0.79 (0.03125)	1.45 (0.057)	Not Detected
C	1.6 (0.0625)	1.51 (0.0595)	Not Detected
C	3.18 (0.125)	1.61 (0.0635)	Not Detected
C	4.76 (0.1875)	1.60 (0.063)	Not Detected
D	0.79 (0.03125)	1.96 (0.077)	Not Detected
D	1.6 (0.0625)	2.08 (0.082)	Not Detected
D	3.18 (0.125)	2.10 (0.0825)	Not Detected
D	4.76 (0.1875)	2.10 (0.0825)	Not Detected

Preliminary data on the bottom-drilled hole standard plate was acquired with the optimized flex probe (FET-3427). A magnitude C-scan image acquired at 400 kHz using the updated flex probe is shown in Figure 5.10. An analysis of detection capability was performed that compared two of the flex probes featuring the optimized design. A summary of these examinations is provided in Table 5.3. The results are presented by row as the depth ranges here from row A to D, and the results show the non-detection of row D. The design drawing of the plate is provided in Figure 4.15 for reference. As expected, the performance of each probe was very similar and only small differences in absolute amplitude were noted. The optimized flex probe performed on par with the Grooveman probe and struggled with the same challenges as the Grooveman probe where the targets in the plate lacked linear features making them more difficult to detect.

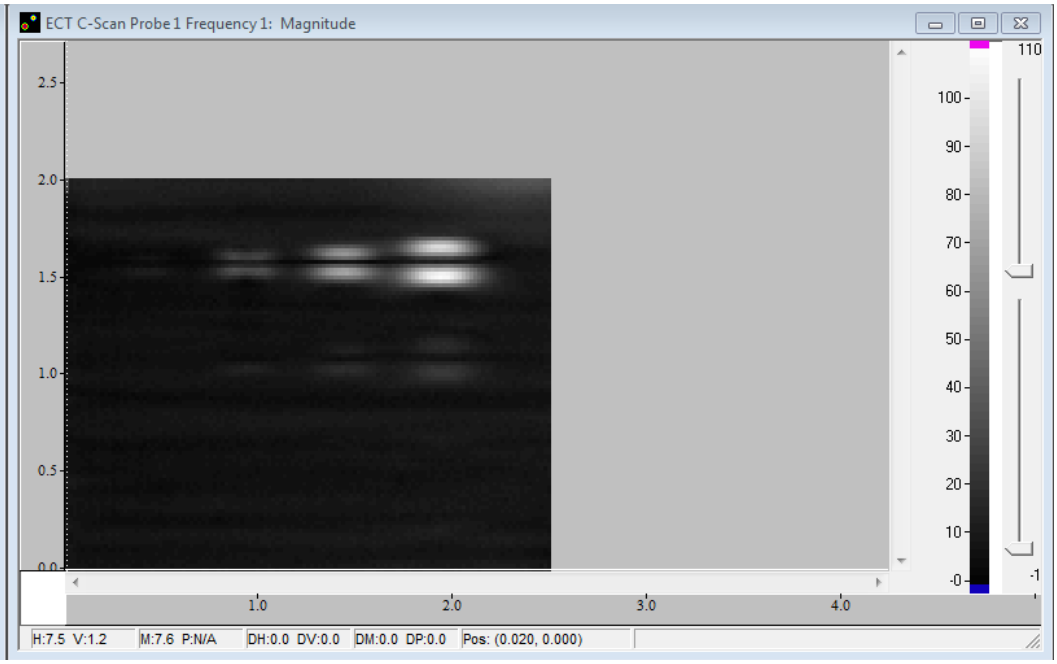

Figure 5.10. C-scan Magnitude Image of the Bottom-Drilled Hole Plate Acquired at 400 kHz Using the Optimized Flex Probe Design

Table 5.3. Summary of Bottom-Drilled Hole Plate Data Acquired with Optimized Flex Probes

Row	Hole Diameter, mm (in.)	Remaining Ligament, mm (in.)	FET 3427 (400 kHz)	
			SN 65966	SN 65967
A	0.79 (0.03125)	0.51 (0.02027)	Detected	Detected
A	1.6 (0.0625)	0.64 (0.0250)	Detected	Detected
A	3.18 (0.125)	0.66 (0.0260)	Detected	Detected
A	4.76 (0.1875)	0.61 (0.0240)	Detected	Detected
B	0.79 (0.03125)	0.91 (0.036)	Not Detected	Not Detected
B	1.6 (0.0625)	1.09 (0.043)	Detected	Detected
B	3.18 (0.125)	1.14 (0.045)	Detected	Detected
B	4.76 (0.1875)	1.12 (0.044)	Detected	Detected
C	0.79 (0.03125)	1.45 (0.057)	Not Detected	Not Detected
C	1.6 (0.0625)	1.51 (0.0595)	Not Detected	Not Detected
C	3.18 (0.125)	1.61 (0.0635)	Not Detected	Not Detected
C	4.76 (0.1875)	1.60 (0.063)	Not Detected	Not Detected
D	0.79 (0.03125)	1.96 (0.077)	Not Detected	Not Detected
D	1.6 (0.0625)	2.08 (0.082)	Not Detected	Not Detected
D	3.18 (0.125)	2.10 (0.0825)	Not Detected	Not Detected
D	4.76 (0.1875)	2.10 (0.0825)	Not Detected	Not Detected

5.3.2 Cold Spray Subsurface Notch Plate

The CS subsurface notch plate was examined with the UniWest flex probe. The smaller width notch that was preserved as a subsurface flaw was detected in all of the ET examinations.

Examinations of the subsurface notch plate with the UniWest flex probe were conducted such that the scanning axis was parallel to the direction of the notches, as shown in Figure 5.11. Because of the rotation of the eddy current coils relative to the body of the probe, the plate was rotated 45° and the 1.02 mm (0.040 in.) thick CS section was re-examined as shown in Figure 5.12. This rotation resulted in parallel alignment of the probe coil and the notches. A schematic used for reconciling this rotation to the resulting image registration is provided in Figure 5.13.

The most promising result of this preliminary work was detection of the smaller-width subsurface notch with the flex probe. Using the flex probe, a strong response was recorded from the subsurface void represented by the smaller notch using both 500 and 300 kHz inspection frequencies.

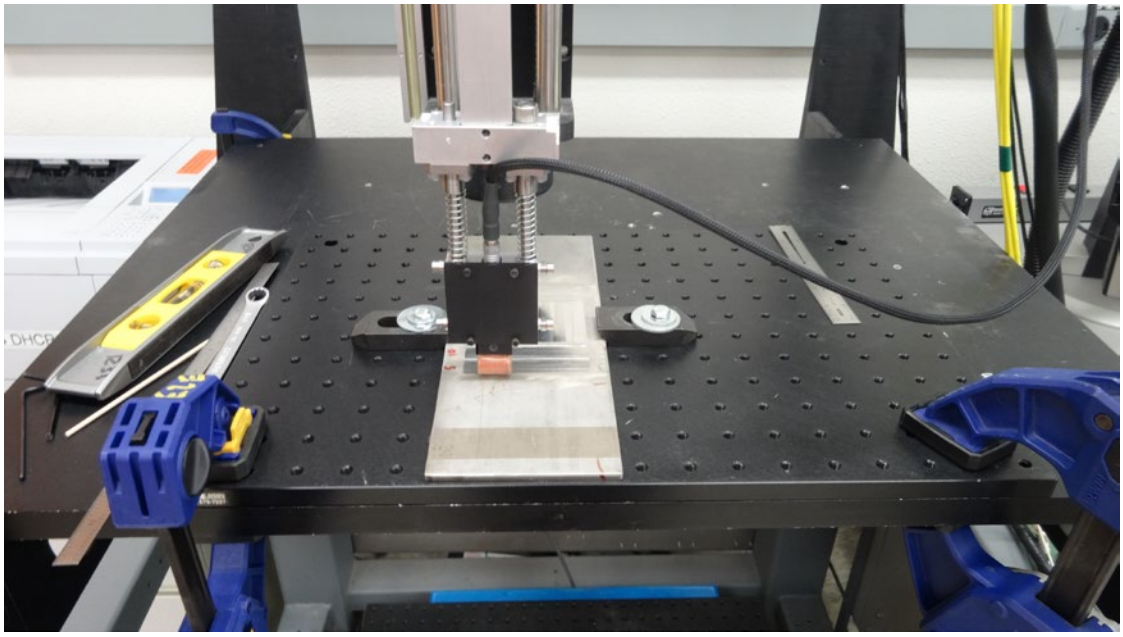

Figure 5.11. Examination of Stainless Steel Plate with Machined Inconel Cold Spray Surface and Two Subsurface Flaws

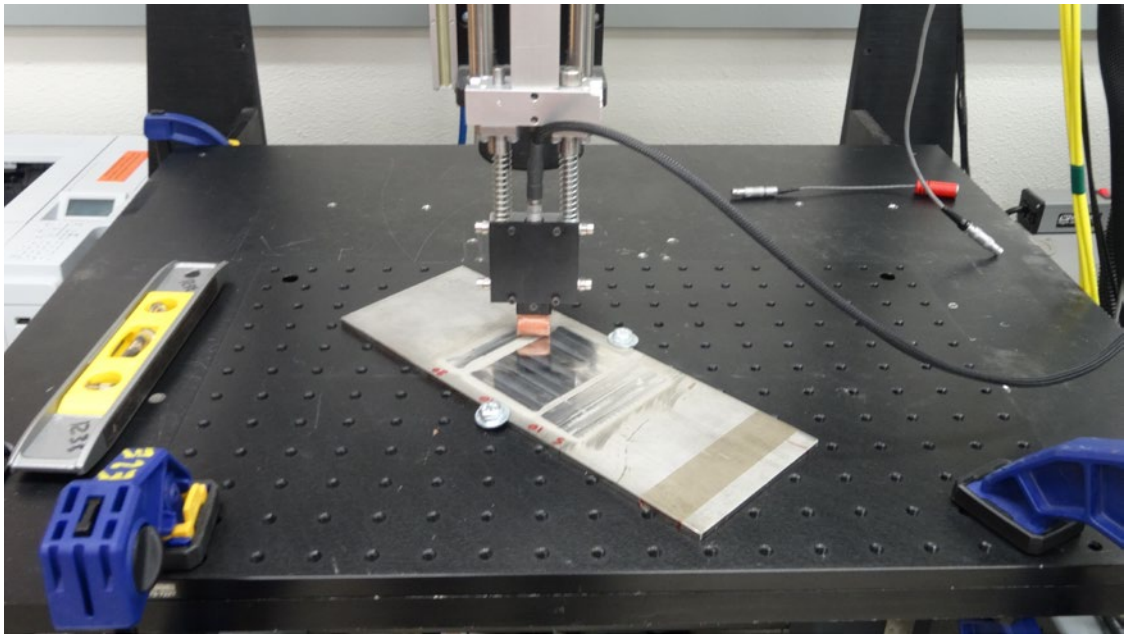

Figure 5.12. Examination of Rotated Subsurface Flaw Plate

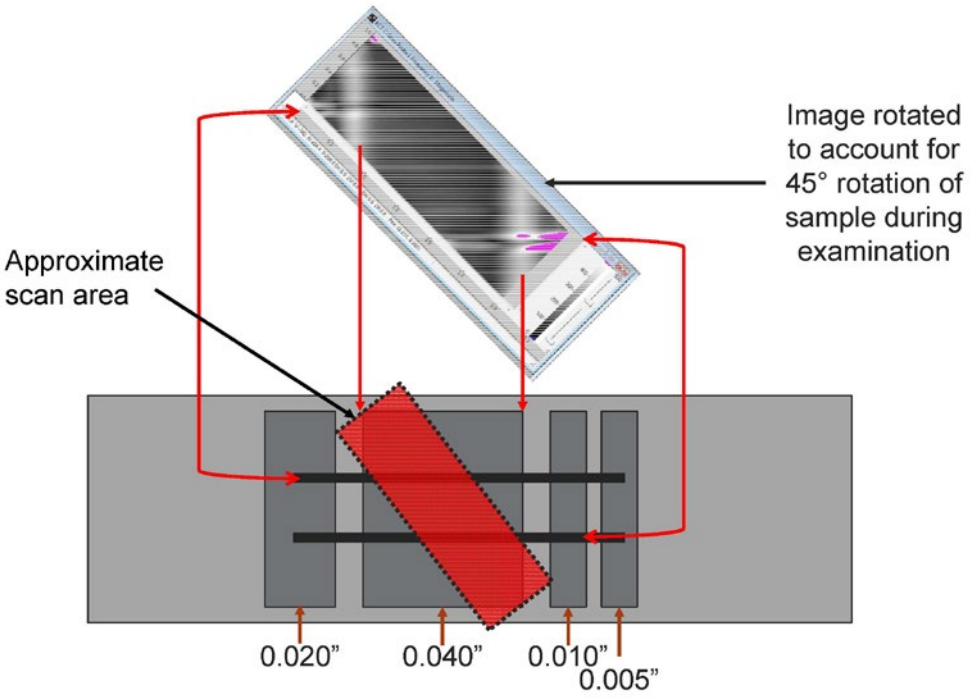

Figure 5.13. Schematic for Interpretation of 45° Off-axis Examination Data of the Cold Spray Subsurface Notches

5.4 Copper Strips

As discussed earlier in the materials and mockups section, when properly applied the copper strips are good surrogates for producing notch-like responses. To accurately produce this type of response, the copper strip width must be tightly controlled. The advantage of this type of surrogate feature simulation is that the adhesive-backed copper strips are easily placed in a variety of orientations on mockups with real welds such as the J-groove welds in the CRDM nozzle specimens. This subsection presents the limited data that was acquired using this copper-strip technique on flat SS plates as well as one of the CRDM specimens.

The final portion of the copper-strip work conducted to date involved placing a copper strip parallel to the J-groove weld such that it was partially in the examination region for the 345°–360° scan. The response from this copper strip is clearly evident in the data as shown in Figure 5.14. The copper-strip response was much larger than the notch response from the Inconel notch plate indicating that further refinement of the notch geometry is necessary to better approximate the notch response. The effort to simulate notch responses using copper strips is inconclusive at this point because this portion of the effort was not completed. The flex probe designs have shown very promising results, and further investigation is required to conclusively determine the detection capabilities of the optimized flex probe near the challenging geometry of the J-groove weld.

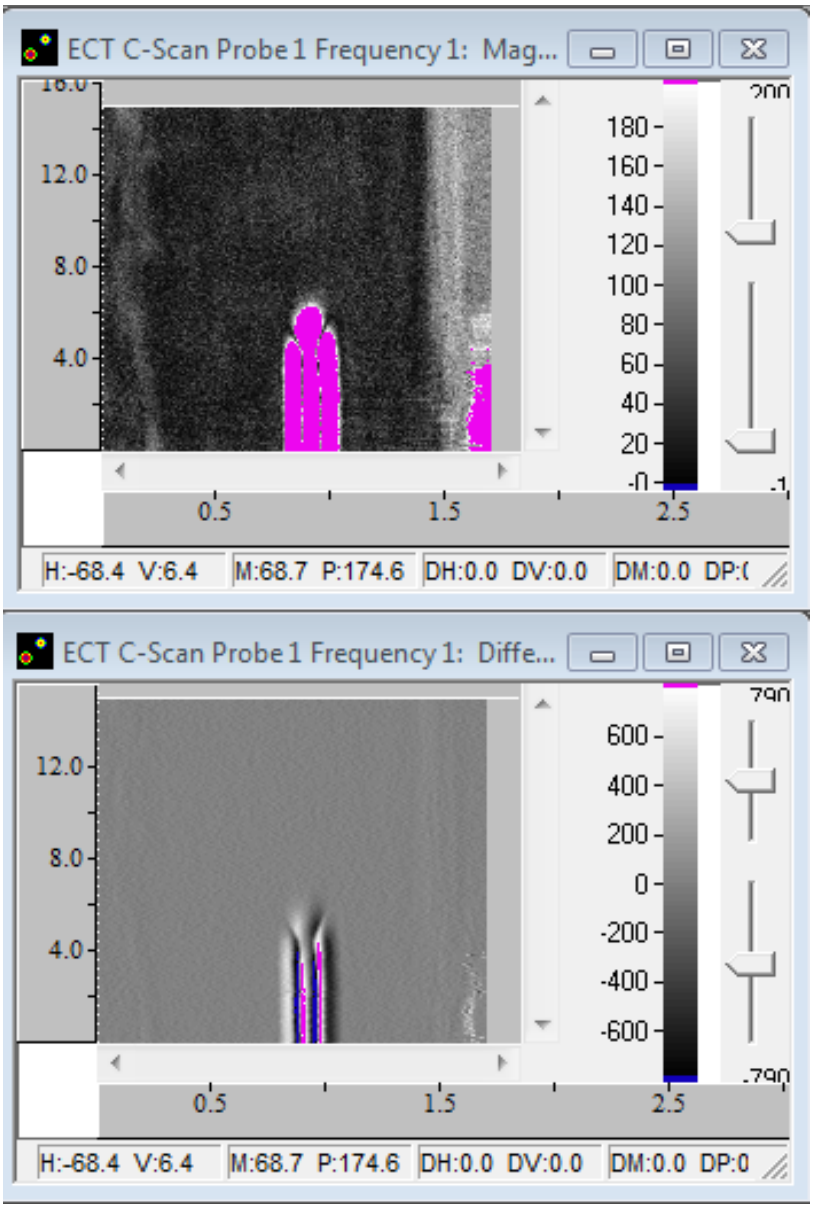

Figure 5.14. CRDM Sample #12 Examination Between 345°–360° where Copper Strip was Applied to the Surface Parallel to the Weld to Represent a Notch Response

6.0 Observations

The following observations are offered based on the compilation of industry field results and laboratory studies:

1. The ASME Code does not have an acceptance standard for ET surface examinations of high nickel-alloy welds, which has limited the use of ET for this application. However, there are numerous documented results from the United States and abroad where ET has been demonstrated through confirmatory testing as a reliable detection technique for both service-induced PWSCC and hot tears. In general, vendor-specific technical justifications have been written to document the capability of ET using ASME Code Section XI, Appendix IV as guidance on how to conduct the experimentation. The minimum flaw detection in a weld reported in the literature is approximately 3 mm (0.12 in.). It is important to note that this detection was on a weld surface ground flush to remove surface irregularities. In general, welds are ground, but one must take caution to assess the weld surface to identify areas that do not accommodate consistent and effective ET probe contact. In addition, surface blemishes, such as scratches and gouges, were readily distinguishable from actual cracks based on analysis guidelines.
2. Laboratory studies at PNNL demonstrated detection of flaws 1.5 mm (0.06 in.) long by 0.4 mm (0.015 in.) deep in plate material. However, there were no welded surfaces with flaws available for evaluation. The ASME Code Section XI, Appendix IV guidelines require flaws in the base metal, heat-affected zone, weld edge, and weld surface for demonstration.
3. ET probes were demonstrated to be capable of detecting near-subsurface voids/inclusions comparable to the ones identified as the root cause of failure in J-groove welds at the South Texas and Palo Verde plants. Subsurface voids were simulated using holes drilled from the back side of plates with various diameters and ligaments. In addition, a cold spray deposition on Inconel 625 was demonstrated to simulate a welded surface.
4. Conventional probe designs were not capable of coupling adequately at the toe of the weld, especially on the downhill side, due to geometric obstructions. However, a special UniWest flexible design bobbin probe detected these subsurface conditions and was able to couple onto the toe of the J-groove weld on the downhill side with very little lift-off noise (these were separate demonstrations because no available samples had subsurface voids in an actual J-groove weld geometry). These results are very promising for a detection method in this region.
5. False positives in field results have been reported based on comparing ET crack-like indications and PT linear indications for a small number of J-groove welds (two at Davis Besse), which used PT as the basis for the final determination. However, PNNL laboratory work on removed nozzles from North Anna Unit 2 showed that DT confirmed ET calls that were not detected by PT. Given the small sample size, it is difficult to draw any firm conclusions; however, it appears that additional ET research needs to be conducted in order to establish a sound technical basis for supporting the expanded required use of ET only for these types of examinations.

7.0 References

ASME. 2009. *Code Case N-770-1, Alternative Examination Requirements and Acceptance Standards for Class 1 PWR [pressurized water reactor] Piping and Vessel Nozzle Butt Welds Fabricated with UNS N06082 or UNS W86182 Weld Filler Material With or Without the Application of Listed Mitigation Activities, Section XI, Division 1*. NY: American Society of Mechanical Engineers. Approved December 25, 2009.

ASME. 2017. *ASME Boiler and Pressure Vessel Code - An International Code*, NY: American Society of Mechanical Engineers.

Berles B. 2014. "Palo Verde BMI Update, March 12th, 2014." Presented at *Regulatory Information Conference*, March 12, 2014, Washington, DC.

Boland AT. 2010. Letter to B Allen. "Davis-Besse Nuclear Power Station Special Inspection to Review Flaws in the Control Rod Drive Mechanism Reactor Vessel Closure Head Nozzle Penetrations 05000346/2010-008(DRS) and Exercise of Enforcement Discretion." October 22, 2010, U.S. Nuclear Regulatory Commission, Lisle, IL. ADAMS Accession No. ML102930380.

Borchardt RW. 2004. Letter to Holders of Licenses for Operating Pressurized Water Reactors as listed in Attachment to the Enclosed Order. "Issuance of First Revised NRC Order (EA-03-009) Establishing Interim Inspection Requirements for Reactor Pressure Vessel Heads at Pressurized Water Reactors." February 20, 2004, Nuclear Regulatory Commission, Washington, DC. ADAMS Accession No. ML040220391.

Crooker P, G White, W Sims and B Rudell. 2014. "Safety Evaluation Request for Additional Information Alloy 600 PWSCC Mitigation by Surface Stress Improvement by Peening (MRP-335, Rev 1)." Presented at *NRC Public Meeting on Peening*, September 9, 2014, Rockville, MD. ADAMS Accession No. ML14254A445. Available at https://www.nrc.gov/docs/ML1425/ML14254A445.pdf.

Cumblidge SE. 2015. "NRC Expectations for Eddy Current Inspections of Peened, Inlayed, and Onlayed Dissimilar Metal Welds." Presented at *Industry/NRC NDE Technical Information, Exchange Public Meeting*, January 13-15, 2015, Bethesda, MD. ADAMS Accession ML15013A279.

Cumblidge SE, SL Crawford, SR Doctor, RJ Seffens, GJ Schuster, MB Toloczko, RV Harris Jr. and SM Bruemmer. 2007. *Nondestructive and Destructive Examination Studies on Removed-from-Service Control Rod Drive Mechanism Penetrations*. PNNL-16628. Richland, WA: Pacific Northwest National Laboratory.

Cumblidge SE, SR Doctor, PG Heasler and TT Taylor. 2010. *Results of the Program for the Inspection of Nickel Alloy Components*. NUREG/CR-7019; PNNL-18713, Rev. 1. Washington, DC: U.S. Nuclear Regulatory Commission.

EPRI. 1988. *Human Performance in Nondestructive Inspections and Functional Tests*. EPRI Report NP-6052. Palo Alto, CA: Electric Power Research Institute (EPRI).

EPRI. 2012. *Materials Reliability Program: Topical Report for Primary Water stress Corrosion Cracking Mitigation by Surface Stress Improvement (MRP-335)*. EPRI Report 1025840. Palo Alto, CA: Electric Power Research Institute (EPRI).

EPRI. 2013. *Materials Reliability Program: Topical Report for Primary Water Stress Corrosion Cracking Mitigation by Surface Stress Improvement (MRP-335, Revision 1)*. EPRI Report 3002000073. Palo Alto, CA: Electric Power Research Institute (EPRI).

EPRI. 2015. *Materials Reliability Program: Topical Report for Primary Water Stress Corrosion Cracking Mitigation by Surface Stress Improvement (MRP-335, Revision 2)*. EPRI Report 3002006654. Palo Alto, CA: Electric Power Research Institute (EPRI).

EPRI. 2016. *Materials Reliability Program: Topical Report for Primary Water Stress Corrosion Cracking Mitigation by Surface Stress Improvement (MRP-335, Revision 3)*. EPRI Report 3002007392. Palo Alto, CA: Electric Power Research Institute (EPRI).

Hsueh K. 2016. Letter to M Sunseri. "Final Safety Evaluation of the Electric Power Research Institute MRP-335, Revision 3, “Materials Reliability Program: Topical Report for Primary Water Stress Corrosion Cracking Mitigation by Surface Stress Improvement [Peening]” (TAC NO. MF2429)." August 24, 2016, U.S. Nuclear Regulatory Commission, Washington, DC. ADAMS Accession No. ML16208A485.

Lareau JP and DC Adamonis. 2003. "Reactor Vessel Head Penetration Inspection Technology Past, Present and Future." In *Conference on Vessel Penetration Inspection, Crack Growth and Repair*, pp. 242-260. September 29-October 2, 2003, Gaithersburg, MD. NUREG/CP-0191. ADAMS Accession No. ML052370241.

Söderstrand H. 2003. *Qualification of Equipment, Procedure and Personnel for Detection, Characterisation and Sizing of Defects in Areas in Nozzle to Safe End Welds at Ringhals Unit 3 and 4*. Report No. 019/03. Sweden: SQC Kvalificeringscentrum AB.

Thomas SE. 2003. "South Texas Project Experience with Alloy 600: Bottom Mounted Instrument Penetration Condition Resolution." In *Conference on Vessel Head Penetration Inspection, Cracking, and Repairs*, pp. 105-108. September 29-October 1, 2003, Gaithersburg, MD. NUREG/CP-0191. ADAMS Accession No. ML053620381. Washington, DC: Nuclear Regulatory Commission.

Weakland D. 2008. Letter to MRP Technical Advisory Group. "MRP 2008-053, St. Lucie Unit 1, Retired Pressurizer Safety “A” Nozzle DM Weld Destructive Examination Report." August 12, 2008, Electric Power Research Institute, Palo Alto, CA. ADAMS Accession No. ML082480225.

PNNL-29113

Pacific Northwest National Laboratory

902 Battelle Boulevard
P.O. Box 999
Richland, WA 99354
1-888-375-PNNL (7665)

www.pnnl.gov